MT-Pallantia Publisher
Journal of Science with Technological Applications
ISSN: 0719-8647

An Approximation to Mechanics and Mass Transport in Polymer-based Hydrogel Systems

José Sebastián López Vélez [1,2]*, Manuel Palencia [1]

[1] *Research Group in Science with Technological Applications (GI-CAT), Department of Chemistry, Faculty of Natural and Exact Sciences, Universidad del Valle, Cali – Colombia.*
[2] *Instituto de Pensamiento Complejo (IPC), Manizales - Colombia.*

Corresponding Author: Manuel Palencia. E-mail: manuel.palencia@correounivalle.edu.co

Graphical Abstract

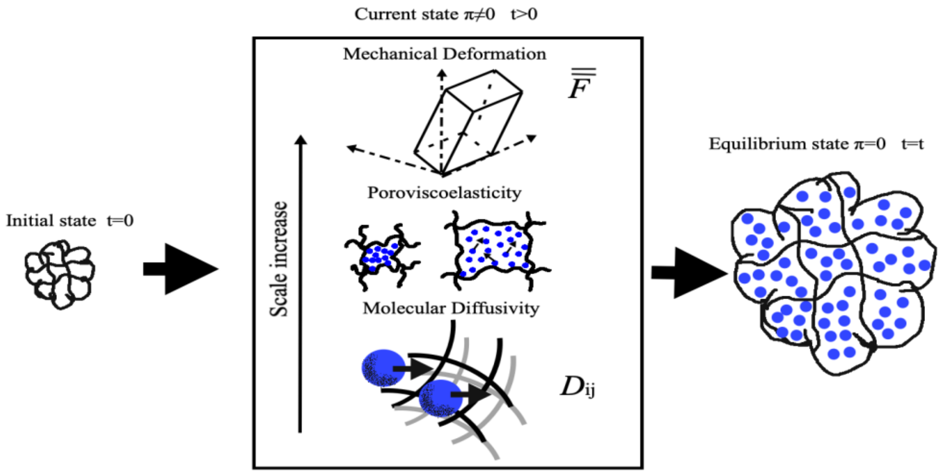

Abstract. The polymer-based hydrogel systems (PHGS) have a wide range of applications in fields like medicine, agriculture, robotic, and others, which has been made these arrangements a promising study area. The poroviscoelasticity behavior present in the PHGSs is associated with the polymeric chain movements and molecular diffusivity of solvents and solutes through the polymeric network due to the actuation of mechanical forces and the chemical potential differences between the structure and the surrounding. In this review paper, we seek to present a bird's eye view of the approaches and concepts, concerted from the thermodynamics and continuum mechanics of solids, that search the description of the PHGS response to the mechanical and chemical surroundings stimulus, punctually the models that consider the volume of the PHGS as a monophasic homogeneous structure where multiple components coexist. In the beginning, the physical-chemical properties of PHGSs are connected with the crosslinking sort of the polymeric network, chemical or physical, and the kind bonds present between polymer chains. Initially, it presents the equilibrium state achieves between the PHGS and the surroundings and where the swelling or shrinking is stopped. Then, it exposes the infinitesimal deformation and the finite deformation approaches, from nonequilibrium thermodynamics, and the poroviscoelasticity approach as an alternative method, that describes the dynamical evolution of the PHGS. Finally, the finite deformation approach is extended to describe the multicomponent mass transfer in PHGS.

Keywords: hydrogels, polymers, poroviscoelasticity, swelling, strain, stress, shrinking, non-equilibrium, equilibrium, mass transfer, PHGS.

Cite as: López Vélez J.S., Palencia M. An approximation to mechanics and mass transport in polymer-based hydrogel systems. J. Sci. Technol. Appl. 10 (2021) 66-91.
https://doi.org/10.34294/j.jsta.21.10.67

Accepted: 2021-08-18 | Published: 2021-08-28 | Paper Number: 067 | Review

Content

1. Introduction

Hydrogels are hydrated systems based on three-dimensional polymer networks characterized to absorb their mass in water many times. Structurally, they can be classified according to polymer structure as: (i) chemically-crosslinked hydrogels (i.e., hydrophilic polymer networks whose chains are covalently linked, therefore, they are insoluble in water and undergo an increase in its volume as a result of water absorption), and (ii) physically-crosslinked hydrogels (i.e., hydrophilic polymer networks whose chains are interacting by ionic forces, dipole-based interactions, hydrogen bonds, physical entanglements of individual polymer chains; or a combination of two or more of the above interactions. They absorb water undergoing an increase in their volume; however, as the chains separate as a result of expansion, their interactions decrease, and then, they are solubilized). Interpenetrated polymer networks (IPNs) are a particular case of physically-crosslinked hydrogels where hydrogel resulting is not soluble, but chains are physically interacting. In other cases, physical entanglements of chains are so strong that polymer matrix is insoluble (e.g., highly-branched polymers characterized by branching with a high degree of polymerization) (Caló and Khutoryanskiy, 2015; Bashir, et al., 2020).

It is essential to differentiate the concept of hydrogel used in polymer chemistry from the concept of hydrogel associated with a multiphase dynamic hybrid system. In the first case, the hydrogel is the polymer, which can pass from a state 1 (dried) to a state 2 (hydrated), and even, depending on the amount of absorbed water, intermediate or critical states could be defined (i.e., unsaturated, saturated, or oversaturated). In any case, under this approach, the hydrogel is a type of polymer. In the second case, the term hydrogel refers only to hydrated polymer since hydrogel behavior is related to polymer structure, but at the same time, it depends on the hydration state. For example, linear poly(acrylic acid), or linear PAA, is a superabsorbent. It is a hydrogel because its behavior in the presence of water is characteristic of hydrogels (i.e., it absorbs water and increases its volume due to hydration). The same occurs with crosslinked poly(acrylic acid) (crosslinking degree = 5 %) but not occurs with highly-crosslinked PAA (crosslinking degree = 50 %), which is like a rigid-sphere with surface hydrophilic groups. However, when PAA is introduced in a non-polar liquid, it does not behave like a hydrogel. Therefore, the structure is not a single criterion to define when a polymer behaves like a hydrogel. In practice, a hydrogel is used to name highly-hydrophilic polymers without considering that the dry and negligible degree of hydration states do not imply a behavior typical of a hydrogel.

In order to avoid confusion, the system defined by hydrated state is, in this review, named to be polymer-based hydrogel systems (PHGSs). Consequently, it is concluded that the basic structure of PHGSs includes a high-hydrophilic polymer phase, water, and other species like counterions or solutes dissolved in the water acting as solvent of them. The chemical potential, interaction strength among polymer structure and water molecules, and the structure's elastic response are the factors triggering the entrance or exit of solvent (i.e., water) and solutes. Here, gels of a non-polymeric nature are not included, resulting from highly-concentrated aqueous solutions of low molecular weight molecules, characterized to be highly hydrophilic and undergoing strong intermolecular interactions in an aqueous medium. Their applications cover a wide range of areas, including medicine, the pharmaceutical industry, agriculture, the food industry, among others (see Table 1).

The dynamic behavior of PHGSs can be characterized by two physical-chemical properties: poroviscoelasticity of polymer structure and the diffusivities of solvent and solutes species. The poroviscoelasticity is the structural property that characterizes the mechanical response of PHGSs, giving rise to the processes of swelling and shrinking, which are time-dependent non-equilibrium processes. The species diffusivities are parameters describing the mass transfer process. The chemical potential differences of the solvent and solutes are the driving force of the mass transfer process, and therefore, it determines the swelling or shrinking of polymer structure. In particular, species diffusion can happen under mechanical equilibrium conditions, but changes of concentration species can result from the differences in the chemical potentials between the inside of the structure and the environment. In addition, PHGSs can also undergo the release of water content by no-diffusive mechanisms which are not controlled by chemical potential. Some examples are the biodegradation, crosslinking and uncrosslinking by changes of dynamic chemical bonds, and hydrolysis of polymer structure; however, these mechanisms are not

Table 1. Some applications of hydrogels

Research field	Polymers and materials	Application	Reference
Agriculture	MMT-PAA	Soil polymer conditioner	(Lerma et al., 2014)
	Polymer based on dextrose, starch, agar, citric acid and sorbitol	Growth medium for plant growth promoting microorganisms	(Garces et al., 2017)
Drug delivery	PEG, PEO, PPO, PDMAEMA, PLGA, PNIPAM, PPF, PCL, PU, POP, PHB, FITC, BAM	Effectively delivering hydrogels inside the body without implantation. Prolonging the release kinetics of drugs from hydrogels. Expanding the nature of drugs which can be delivered using hydrogel-based approaches	(Hoare and Kohane, 2008)
	Porous scaffold-based in alginate with covalently coupled RGD and embedded with particles of iron oxide	An active porous scaffold that can be remotely controlled by a magnetic field to deliver various biological agents.	(Zhao et al., 2011)
	HPMC	To reproduce the hydrogel matrix behavior after drug administration	(Caccavo et al., 2015)
	Collagen, Calcium phosphate and Collagen, Poly(2-hydroxyethylmethacrylate), poly(2-hydroxypropylmethacrylate), poly(acrylic acid), PEG, Urethane polymer, Carbomer 940, Carbomer 980, Gelatin, Alginate, hydroxyethylcellulose, carboxymethylcellulose	Hydrogel drug delivery systems. Control in time and space over drug presentation. Guidelines for rational design of hydrogel delivery systems based in experimental data and clinical translation	(Li and Mooney, 2016)
Food processing	Whey protein isolate (WPI)	Hydrogels induced by preheating solutions of WPI with $CaCl_2$	(Barbut and Foegeding, 1993)
Microfluidics	Polymer based on acrylic acid, 2-hydroxyethyl methacrylate, Ethylene glycol dimethacrylate and photoinitiator	The fabrication of active hydrogel components inside microchannels via direct photopatterning of a liquid phase	(Beebe et al., 2000)
	PNIPAM, PNIPAA	Develop and applications in remote-controlled (RC) nanocomposites hydrogels	(Satarkar et al., 2010)
	Alginate, PLGA, Chitosan, PPDO-co-PCL-b-PEG-b-PPDO-co-PCL, 4-HBA, PVA, PU, PNIPAA, PEG, Silica, TPGDA, PBA-PAA, PFPE, AHPCS, Acrylamide, Agarose, Gelatin, Pluronic, PGS, Collagen, Silk fibroin, Methylated hyaluronic acid.	Current development of microfluidic-based fabrication techniques for the creation of fibers, particles, and cell-laden hydrogels	(Chung et al., 2012)
	Theoretical polymer	pH-sensitive hydrogels for microfluidic flow control systems	(He et al., 2012)
Oilfields	Theoretical polymer	PHGS has been modeled on the exterior surface of a metallic tubing that imbibes a solvent and swells. The objective is redistribution of the hydrogel, building up the sealing pressure to the state of equilibrium	(Cai et al., 2010)
Pharmaceutics	Poly(sorbitol citrate)	Controlled-release of bioactive substances	(Palencia et al., 2017a)
	Crosslinked PAA-Starch	Controlled-release of cysteamine-AgNPs	(Palencia et al., 2017b)
Soft machines	PVA / PAA, PNIPAA	Piezoresistive sensors use pH-sensitive hydrogel to generate a deflection of the silicon membrane within a sensor chip that is translated to an output voltage signal	(Gerlach et al., 2005)
	HEMA:DMAEMA, PHEMA-co-MAA, PAAm-PCCA, PVA – PAA, poly(AA-co-IOA), PMAA-PEGDMA, AAm-DMAEMA	Physical background of sensors based in the stimulus-response of pH-sensitive hydrogels	(Richter et al., 2008)
	SAM	Dielectric elastomers study	(Suo, 2010)
Tissue engineering	Collagen, Gelatin, Hyalluronate, Fibrin, Alginate, Chitosan, PAA, PEO, PVA, Polyphosphazene, Polypeptides	Tissue engineering materials study	(Lee and Mooney, 2001)

Agarosa – cysteine, GRGDS	A photolabile 3D hydrogel is generated like a matrix for guided axonal growth. The method proposes the immobilizing biomolecules in 3D matrices that offering a solution to construct scaffolds with programmed spatial features for tissue engineering applications.	(Luo and Shoichet, 2004)
Chondroitin Sulfate, Hyaluronic acid, Chitosan, Cellulose, Alginate, Collagen, Gelatin, Elastin, Fibroin.	Hydrogels based on natural polymers with different applications in tissue engineering	(Van Vlierberghe et al., 2011)
Gellan gum	Gellan gum hydrogels as materials for applications in tissue engineering	(Ferris et al., 2013)

PSS: poly(styrene sulfonate); MMT: Montmorillonite; HPMC: hydroxypropyl-methylcellulose; PEG, poly(ethylene glycol); PEO, poly(ethylene oxide); PPO, poly(propylene oxide); PDMAEMA, poly(dimethylaminoethyl methacrylate); PLGA, poly(lactide-co-glycolic acid); PNIPAM, poly(N-isopropyl-acrylamide); PPF, poly(propylene fumarate); PCL, poly(caprolactone); PU,poly(urethane); POP, poly(organophosphazene); PHB, poly(R-3-hydroxybuty-rate); FITC, fluorescein isothiocyanate; BAM, N-tertbutylacrylamide; .AgNPs: Silver nanoparticles; RGD: Arginine – glycine – aspartic acid; PNIPAA: poly(N-isopropylacrylamide); PLGA: poly(D,L-lactic-co-glycolic acid); PPDO-co-PCL-b-PEG-b-PPDO-co-PCL:poly(p-dioxanone-co-caprolactone)-block- poly(ethylene oxide)-block-poly(p-dioxanone-co-caprolactone); 4-HBA: 4-hydroxy butyl acrylate; PVA: poly(vinyl alcohol); TMPTA: tri(methylol propane triacrylate); PEGDA: poly(ethylene glycol) diacrylate; TPGDA: Tripropyleneglycol diacrylate; PBA-PAA: poly(butyl acrylate)-b-poly(acrylic acid); PFPE: perfluoropolyether; AHPCS: allylhydridopolycarbosilane; PGS: poly(glicerol sebacate); PDMS: polydimethylsiloxane; PAA: poly(acrylic acid); HEMA:DMAEMA: 2-hydroxyethyl methacrylate - N,N-dimethylaminoethyl methacrylate; PHEMA-co-MAA: poly(hydroxyethyl methacrylate-co-methacrylic acid); PAAm-PCCA: poly(acrylamide) - polymerised crystalline colloidal array; poly(AA-co-IOA): poly(acrylic acid-co-isooctyl acrylate); PMAA-PEGDMA: poly (methacrylic acid)-Poly(ethylene glycol) dimethacrylate; AAm-DMAEMA: acrylamide - N,N-dimethylaminoethyl methacrylate; SAM: soft active material; GRGDS: glycine– arginine–glycine–aspartic acid–serine.

discussed in this review (Oliveira et al., 2004; Cai et al., 2010; Cai and Suo, 2011; Garces et al., 2017; Palencia et al., 2017a, Palencia et al., 2017b).

Two physical approaches have been developed to understand the swelling hydrogels process used depending on the study objective. First, multi-phase approaches were developed based on the hypothesis that the polymer network and solvent are two phases. The Newton second law was used to generate models that include the reproducing friction, relative motion, and phases' viscosity (Tanaka et al., 1973; Tanaka and Fillmore, 1979; Peters and Candau, 1986; Peters and Candau, 1988). Other models were developed treating the system as two-fluid using phenomenological hydrodynamic relations to associate the stress and the gel composition (Doi and Onuki, 1992; Yamaue and Doi, 2004; Yamaue and Doi, 2005; Doi, 2009; Calderer et al., 2010). These models require non-physical-based parameters and used several numbers of partial differential equations (PDE's). Also, these theories have a great capacity to detail the description of gel properties (Caccavo, et al., 2017). Nonetheless, they cannot be easily incorporated into the numerical simulations that study the material response in complex situations, however, these are not included in this work. This sort of approach does not include in this work. Second, the mono-phase point of view was developed to approaches the polymer-solvent system swelling like a unique continuous phase where multicomponent coexist (Durning and Morman, 1993; Hong et al., 2008). The more unified theories and popular has a thermodynamical framework coupling the large deformation theory with the mass transport diffusion. Thanks to the stronger thermodynamic based, this model requires fewer PDEs and can be easily adapted to numerical simulations that could reproduce the material's behaviors (An et al., 2010; Chester and Anand, 2010; Duda et al., 2010; Hong et al., 2010; Chester and Anand 2011; Chester, 2012; Lucantonio et al., 2013). All approaches discussed in this work are of this nature.

Thus, it could consider a hydrogel system like an elastic homogeneous solid submerged inside a fluid medium. Hence, it is necessary to select a reference frame to study the changes suffering to the hydrogel. In systems to involve solids, fluids, or both exist, two coordinated systems address them. First, the Lagrangian approach uses material coordinates that establish an initial reference state X_K to measure the current variation to suffer the system x_i. Second, the Eulerian method uses spatial coordinates (x_1, x_2, x_3, t) in a control volume to measure the entry and exit of mass and energy through the boundaries. Both reference frames have been adopted in the hydrogel study and are necessary to include in the approaches that treat this work (Snoeijer et all., 2020). Nevertheless, the Lagrangian approach is more valuable when dealing with the coupling of the mass transport with solid mechanics is also challenging to analyze nonlinear solids in spatial coordinates (Caccavo and Lamberti, 2017).

The above shows that a complete understanding of mechanical and mass transfer properties from a consistent thermodynamical and kinetical framework is vital for designing, applying, and optimizing functional PHGS. In this work, concisely, some of the more recent coupled models developed between the thermodynamic and continuum solid mechanics applied on the hydrogel field are shown. Initially, the nature of the physical-chemical properties in the PHGS system regarding the cross-linking and bond types are exposed. In the same section, the poroviscoelasticity response of the PHGSs is explained and is associated with the polymeric chain movements and molecular diffusivity. Following, the equilibrium state that reaches the PHGS is described in terms of thermodynamical equilibrium and the energy balance. Soon, the infinitesimal and the finite deformation approaches applied on the PGHS with a single solvent diffusion and developed from the non-equilibrium thermodynamics are presented. In addition, it is also shown the principal models allowing to compute the Helmholtz free energy due to the elastic, mixing process, and other energy forms. Next, a single diffusion poroviscoelastic approach is described. Finally, the finite deformation approaches developed from the non-equilibrium thermodynamics are present in terms of multicomponent mass transfer. In the same section, the ways to establish the mass transfer regimen, the molar flux calculation, and the diffusivity calculation under the influence of polymeric networks are included.

2. The nature of the physical-chemical properties in PHGS

Crosslinking refers to chemical linking points of two or more chains or segments of polymer chains. When crosslinking is defined from physical interactions, they are not localized in one atom or atom group, but they are a result of interaction field on the space, usually electrostatic in nature. Mechanical crosslinking can be identified in the interpenetrate polymer network (IPNs), where two networks are not chemically linked, but they cannot be physically separated. It is essential to clarify that physical crosslinking is a form to name physical interactions occurring in the material and not corresponds to "true" crosslinking points. Whereas chemical crosslinking is a result of chemical transformations, physical crosslinking depends on the interaction strength between polymer chains and, consequently, on the nature of their functional groups, the intermolecular distance, which is directly associated with the polymer concentration, and chemical environment affecting the interacting groups and the properties of the chains (Maitra and Shukla, 2014; Palencia et al., 2014; Lerma et al., 2017). Effects of crosslinking type on hydrogel properties are summarized in Table 2.

From Table 2 can be concluded that the mechanical properties of hydrogels have a strong dependence on the nature of the crosslinking bonds. As it was previously indicated, crosslinking can be chemical (i.e., covalent, coordinate, and dynamic-covalent bonds) or physical (i.e., by electrical field interactions and mechanical interactions) (Caccavo et al., 2017a; Picchioni and Muljana, 2018). Some examples in the hydrogel context are summarized in Table 3.

Table 2. Effects of crosslinking and the crosslinking degree (CLD) on hydrogel properties (Maitra and Shukla, 2014; Palencia et al., 2014; Lerma et al., 2017).

Crosslinking	Effect	Comments
Chemical	Solubility	Solvation occurs in the particles, but these cannot be spatially reorganized to achieve a homogeneous distribution and form a liquid dissolution.
	Swelling	At a high CLD, polymer chains can be strongly hydrated, but the small interchain space impossibilities the inclusion of water molecules; therefore, the swelling is minimal. On the contrary, at intermediate and low crosslinking degrees, in common, swelling is increased. In general, if crosslinking degrees increase, then swelling decreases.
	Increase in atom number	The inclusion of a crosslinker has been associated with the chemical incorporation of new atoms. However, the system is described by the size of the particle instead of molecular weight. Therefore, an effect on molecular weight cannot be defined. An increase in the number of atoms associated with an inert crosslinker leads to two situations: (i) a greater crosslinker size implies that the linking points are more distant and therefore the swelling is favored; and (ii) when the increase in the number of atoms is associated with a higher concentration, then linking points will be closer and therefore the swelling is disfavored.
	Mechanical properties	High CLD: In general, the material's mechanical properties are increased (hardness and mechanical resistance). Consequently, polymer particles can be packed in column systems, depending on their size, dispersed under stirring, and synthesized with defined forms depending on the synthesis methods. Mechanical properties decrease as CLD is decreased. The material is more flexible, the less the crossover, and the greater the distance between the attachment points.
	Thermal properties	Hydrogels behave like thermostable materials; therefore, they cannot melt. The fusion involves the supply of energy and the reorganization of the chains to achieve greater molecular mobility. In these materials, the observed process will be thermal degradation at high temperatures.
Physical	Solubility	Hydrogels are soluble when the physical interaction allows the rearrangement of the chains. This is usually associated with voluminous side chains, which generate a greater intrachain volume. However, this reorganization depends on the degree of branching and length of the branches, since the higher the values, the greater the restriction of molecular mobility. An exception is the IPNs. Solubility is only observed when hydrogels are immersed in excess of solvent.
	Swelling	The polymer structure does not limit swelling. In these materials, swelling is observed at low solvent contents. As solvent content is increased, then hydrogel undergoes a gel behavior, i.e., swelling is stopped, but intermolecular interactions are strong; consequently, the system is a fluid characterized by high viscosity, with a gel-like behavior.
	Mechanical properties	A minor effect of physical crosslinking on mechanical properties is expected in comparison with chemically crosslinked hydrogels. These materials cannot be packed, and defined forms can only be achieved by using auxiliary materials (e.g., containers).
	Thermal properties	Physically crosslinked hydrogels can be found, excepting the IPNs and highly-branched materials where molecular reorganization is not possible.

Table 3. Examples of crosslinking type in hydrogels

Crosslinking type	Bond type	Example	Applications and remarks	References
Chemical	Covalent	HG based on poly(sorbitol citrate)	Controlled-release of bioactive substances. The nature of crosslinking points is esters groups from hydroxyl groups from sorbitol and carboxylic acid groups from citric acid. Biodegradable material. Low molecular precursors.	(Palencia et al., 2017a)
		HG from crosslinked PAA-Starch	Controlled-release of cysteamine-AgNPs. The nature of crosslinking points is esters groups from hydroxyl groups from sorbitol and carboxylic acid groups from PAA. Partially biodegradable material. High molecular precursors.	(Palencia et al., 2017b)
	Coordinate	Alginate HGs	Drug delivery vehicles in cancer treatment and wound dressing. Biobased HG from biopolymer. HG's network is formed from calcium or magnesium salts which can be used as ionic crosslinker (egg-box model). Though crosslinker is defined to be ionic in nature, the interaction with polymer is by coordination of divalent cation.	(Abasalizadeh et al., 2020)
		HGs containing dopamine, and HGs based on cathecol-DMA	Tris-complex crosslinking of the metal-ligand complex between Fe^{3+} ions and catechol groups is controlled by changes of pH. It is identified as a potential material for designing soft actuators and robots.	(Liao et al., 2017; Pichioni and Muljana, 2018)
	Dynamic-covalent	HGs based on acylhydrazone and disulfide bonds	HGs are characterized to show environmental adaptive self-healing ability and dual responsive sol-gel transitions. Crosslinking points are based on disulfide bonds (-S-S-)	(Deng et al., 2012; Pichioni and Muljana, 2018)
Physical	Ionic	HGs based on chitosan and sodium alginate	Polyelectrolyte complex from one biopolymer (alginate) and a biobased polymer (chitosan) Potential applications as flexible solid-state supercapacitors	(Zhao et al., 2018)
	Hydrogen bond	HGs based on chitosan and PVA	HGs are obtained from one biobased polymer and a synthetic polymer. Biocompatible drug delivery systems. It is produced a strong interaction among electronegative atoms of functional groups on polymer chains (N and O for chitosan, and O for PVA) and hydrogen atoms linked to electronegative atoms from another polymer chain (-O-H and -N-H).	(Berger et al., 2004)
		HGs from PVP and tannic acid	HGs were named as "coacervate HGs". These shown reinforced molecular interactions attributed to the presence of galloyl groups with a high density, and they were prepared by simple mixing.	(Gyum-Nam, 2019)
	Mechanical	HGs based on IPNs from konjac glucomannan and PMAA	MAA was polymerized in side of konjac glucomannan using MBAm as crosslinker. HGs showed a sensitive response to environment pH value respect to degree of swelling. It is proposed as carrier candidate for colon-specific drug delivery.	(Xu et al., 2013)

HGs: Hydrogels; DMA: Dimethylacrylamide; PVA: Poly(vinyl alcohol); PVP: poly(N-vinylpyrrolidone); PMAA: poly(methacrylic acid); MBAm: Methylenebisacrylamide

3. Poroviscoelasticity in PHGSs

In PHGSs, the poroviscoelasticity phenomena are the associative response between viscoelasticity and poroelasticity behaviors due to the solvent molecules' migration and movement, as shown in Figure 1. The viscoelasticity is generated by the configurational variations or deformations related to molecular sliding between polymer chains and rotational of the chemical bonds among the parts of an individual polymeric section. In this conformational event, the PHGS shape changes happen at constant volume because the solvent molecules have a "short-range" motion. The poroelasticity is produced by a "long-range" motion of the solvent molecules where its numbers are not conserved locally. In this case, the volume swelling or shrinking results from the differences in solvent chemical potential between this and surroundings (Hu and Suo, 2012; Wang and Hong, 2012; Caccavo and Lamberti, 2017; Caccavo et al., 2018).

The viscoelasticity and poroelasticity are material-specific properties and time-dependent terms. The viscoelasticity is related to the viscoelastic relaxation time τ_v, which is specific for each polymeric material and independent of the specific length or any macroscopic observation. Here, the specific length refers to experimental geometry, and it is much larger than any microscopic or molecular scale (Schapery, 1997). So, the τ_v is a time scale associated with a short-range molecular movement, as said above. The poroelasticity is characterized by the effective diffusive coefficient D_{ij} of the solvent in the polymeric matrix. A unique length scale that gathers both terms L_c, denotes the distance of spread of solvent molecules within an equivalent time to the viscoelastic relaxation, as shown in equation (1). This length is exclusive for each pair polymer-solvent and independent of any specific length (Hu and Suo, 2012). Experimental measurements of τ_v can be done using the indentation method (Cai, et all., 2010; Hu, et all., 2010; Hu, et all., 2011; Bush, et all., 2015), the compression

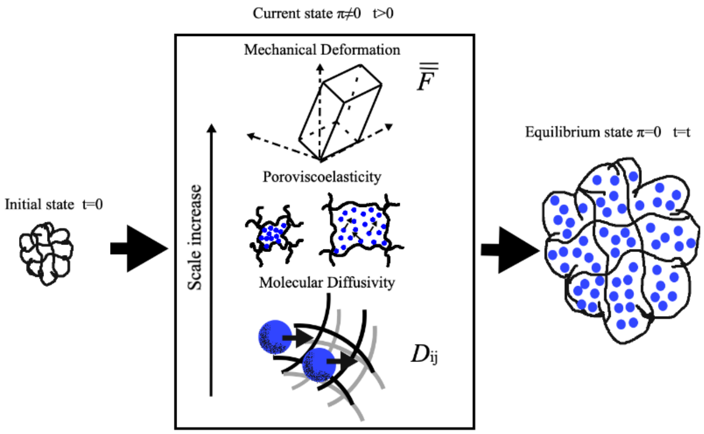

Figure 1. A graphical representation of viscoelasticity and poroelasticity. In the first behavior, the polymeric chains and the network suffers conformational rearranges, and the solvent molecules have a "short-range" movement. In the second behavior, the solvent molecules have a "long-range" movement (adaptation from Hu and Suo, 2012).

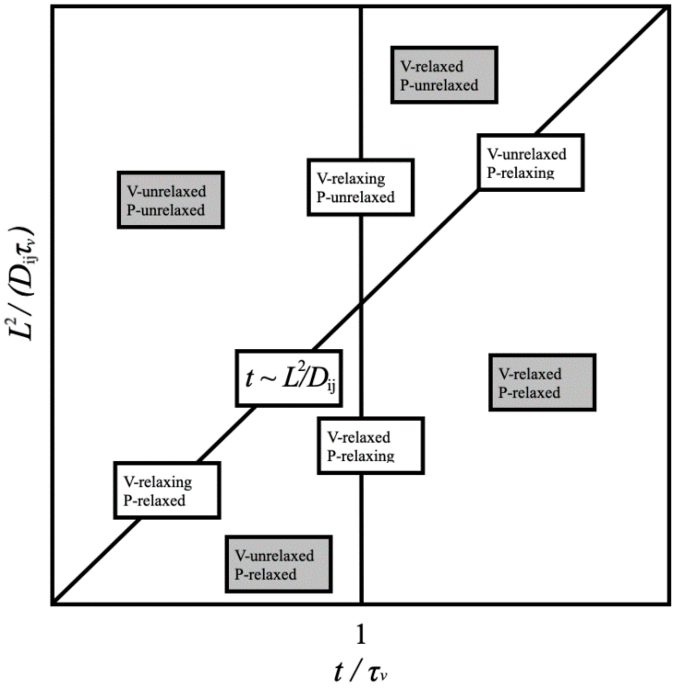

Figure 2. Schematic representation of different limiting conditions of viscoelasticity (V) and poroelasticity (P) where the square of the length $D_{ij}\tau_v$ is a function of the time τ_v (adaptation from Hu and Suo, 2012).

test (Zhao, et all., 2010), and other techniques like atomic force microscopy and nanoindentation (Rosenbluth, et all., 2008; Charras, et all., 2009). In some cases, these experimental procedures permit the measurement of the L_c and identify the viscoelasticity and the poroelasticity behaviors separately (Strange et all., 2013).

$$L_c = \sqrt{D_{ij}\tau_v} \qquad (1)$$

Experimental values of time t and length L^2 can be compared with known τ_v and L_c for a specific material to determine the advances of viscoelasticity and poroelasticity process, as shown in Figure 2, where any point inside the diagram represents a pair of (t, L^2). The vertical line denotes the time of viscoelastic relaxation $t \sim \tau_v$,, and the inclined line represents the time and the length of poroelastic relaxation $t \sim L^2/D_{ij}$. The graphic shows four regions in grey color boxes where indicate that the process must be started (unrelaxed) or finished (relaxed). The limits of the regions in white color boxes express the dominant behavior in the rate of changing (relaxing) and the other process that must be started (unrelaxed) or finished (relaxed) (Hu and Suo, 2012).

4. Equilibrium thermodynamics

From a macroscopic point of view, the swelling relates to the mass quantity of solvent that an amount of dry polymer can absorb in the equilibrium state. So, the swelling mass ratio q_F compares the mass of a hydrated PGHS after arriving at the equilibrium m_{hg} with the initial dry polymer mass m_{dg}. With this, a limited hydrogel quantity has reached the equilibrium when q_F is constant.

$$q_F = \frac{m_{hg}}{m_{dg}} \qquad (2)$$

It can also say that the hydrogel reaches the state of swelling equilibrium with the solvent bulk when the solvent chemical potential inside the PGHS structure $\Delta\mu_1^G$ is balanced with the solvent chemical potential $\Delta\mu_1^S$. The subscript 1 is referred to the solvent and *2* for the polymer network, as seen in equation (3). Equation (4) shows the same equilibrium definition in terms of osmotic pressure π, where is v_1 the solvent's molar volume. Osmotic pressure determines whether the hydrogel is swelling or shrinking, which the solvent is going in or going out of the hydrogel until the osmotic pressure arrives at zero value in the equilibrium state (Okay et al., 1998).

$$\Delta\mu_1^G = \Delta\mu_1^S \qquad (3)$$

$$\pi = -\frac{\mu_1^G - \mu_1^S}{v_1} = 0 \qquad (4)$$

Now, consider a hydrogel sample that exchanges solvent molecules n_s with the surroundings and has a constant number of polymer segments (monomers) n_m, and crosslinking molecules n_c. It is known that the total volume of a hydrogel system is not exactly the algebraic sum of individual components volume. Nevertheless, it is assuming that the volume changes due to a mixture of polymeric network and solvent are neglect because the change due to swelling is enormous. Thus, it is conceivable to approximate that the sum of volume monomer and solvent's total volume estimates neglect the small crosslinking volume (Cai and Suo, 2012).

$$V \approx n_s v_s + n_m v_m \qquad (5)$$

Two thermodynamical potentials could be considered to know the hydrogel system's change: the Gibbs representation $G(T, P, n)$ and the Helmholtz representation $A(T, V, n)$.

The change in the thermodynamical potential is generated by variations in the constraints described by the *Gibbs - Duhem* equation as seen for both representations in the equations (6) and (7). The Gibbs representation is compound to $G(T, P, n_s, n_m, n_c)$ which the variation in the pressure changes the volume. The pressure can alter the total volume value, but this is only happening to the solid or liquid system at very high pressures. Thus, the selected thermodynamical potential is the Helmholtz representation $A(T, V, n_s)$ for the PGHS system, shown in equation (7), further including the volume approximation done by the equation (5).

$$dG = -SdT + VdP + \mu dN \qquad (6)$$

$$dA = -SdT + PdV + \mu dN \qquad (7)$$

Hence, equation (8) defines the solvent's chemical potential as the Helmholtz free energy change concerning the solvent concentration variation c_1 at a constant temperature, volume, and the other species concentration (Dimitriyev et al., 2019).

$$\mu_1 = \left(\frac{\partial A}{\partial c_1}\right)_{T,V,n_{j\neq 1}} \qquad (8)$$

At this point, the integral definition of energy balance expresses the equilibrium state for a PGHS volume with the surroundings.

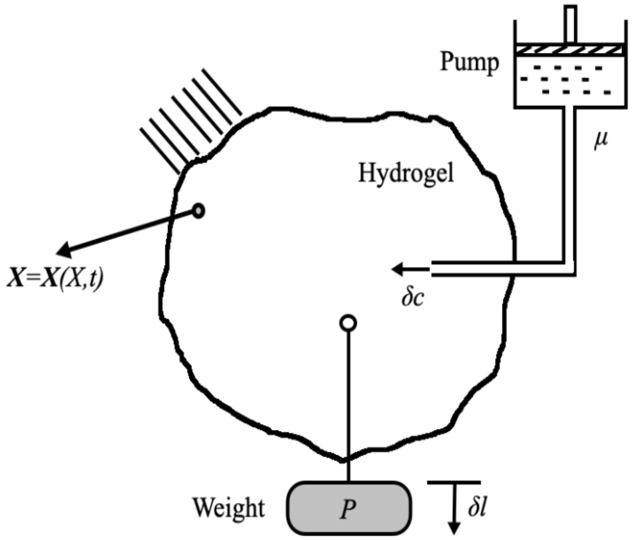

Figure 3. A PGHS body under effects of the chemical load due to the entrance of solvent molecules by the action of the pump, mechanical load for the effect of hanging weight, and traction by friction (adaptation from Hong et al., 2008).

The total Helmholtz free energy change δA over the hydrogel total volume dV is due to by: (i) any mechanical force applied over the hydrogel volume B_i that is represented by the hanging weight; (ii) the traction exerted by the friction over hydrogel surface T_i; (iii) the chemical potential μ_r to the r species adding or extracted to the hydrogel volume that is represented by a hypothetical pump, as shown in Figure 3 (Hong et all., 2008). The concentration c_r of r species considers the solvent, ion charge species (pH-sensitive hydrogels), possible analytes (separations systems), and species that participate in photochemical reactions (photo-thermal gels) (Liu et al., 2015). Other forces that exert influence over the system, like electromagnetic, can be added to the balance (Hong et all., 2010).

$$\int_V \delta A dV = \int_V B_i \delta x_i dV + \int_A T_i \delta x_i dA + \sum_r \left(\mu_r \int_V \delta c_r dV\right) \qquad (9)$$

5. Non-equilibrium thermodynamics

5.1. Infinitesimal deformation with a single solvent diffusion

To understand the hydrogel nonequilibrium process has used the concept of a homogeneous state. This approach accepts the hypothesis of infinitesimal deformation (ϵ_{ij}) used to propose the fundamental equation. This development can be considered a simplification used to understand the large deformation theory that will be present in the next section.

The homogeneous state considers the hydrogel system as a sum of many infinitesimal pieces laterally attached to one other and can evolve individuals in time to homogeneous way. In this scheme, hydrogel pieces' communication is defined by kinematic of deformations, balances forces, the mass balance of solvent, and solvent diffusion. Thus, it is possible to establish the setup that is constituted by a small homogenous piece of hydrogel, a set of external forces, molecules of solvent, and the environment.

Some constraints of this model are that the solvent is the unique molecular species spreading in the volume without taking into account other species, and second, the system is isothermal. In the reference state, the hydrogel is not subject to external force, and the environment has a fixed solvent chemical potential μ_0. The system's physical representation is considered under the nonequilibrium thermodynamics models given δA be the Helmholtz free energy difference between the reference state and the current moment. Besides, it regards the chemical load $(\mu - \mu_0)$ and mechanical load σ_{ij} which causes an infinitesimal deformation $\delta\epsilon_{ij}$. Equation (10) describes the composite thermodynamical system where the equality represents the reversible changes around the equilibrium state and the inequality the irreversible changes.

$$\delta A - \sigma_{ij}\delta\epsilon_{ij} - (\mu - \mu_0)\delta c_1 \leq 0 \qquad (10)$$

Moreover, a rheological model can describe the change in the Helmholtz free energy of the system. The complete setup is represented by two springs α, β and one dashpot $\hat{\beta}$ as shown in Figure 4. Here, the independent variables are considered the strain of the spring α and the dashpot $\hat{\beta}$ defined in equation (11). The hydrogel is a soft matter system subject to small stress, so it has been possible to consider the polymeric chain and solvent molecules as incompressible parts. Instead, it is possible to relate the volumetric change of the hydrogel by the variation of the solvent molecules inside the structure as shown in equation (12), where Ω is the volume per solvent molecule

$$A = A\left(\epsilon_{ij}, \hat{\epsilon}_{ij}\right) \qquad (11)$$

$$\epsilon_{kk} = \Omega\left(c_1 - c_{1_0}\right) \qquad (12)$$

Considering the above can describe the energy interactions experience by the system as shown in equation (13). When the dashpot is constrained $\delta\hat{\epsilon}_{ij} = 0$, the two spring is deformed to equilibrate the load over the system, and the change in the chemical potential represented equally (14). When the spring α is constrained $\delta\epsilon_{ij} = 0$ the system needs to dissipate energy through the subsystem form with the dashpot and the spring β that is representing by the inequality (15). The δ_{ij} is the Kronecker delta where $\delta_{ij} = 1$ when $i = j$ and $\delta_{ij} = 0$ when $i \neq j$ (Holzapfel, 2002). The equation (14) is an equation of state, and the inequality (15) is a kinetic time-depended, which how the system dissipates energy through the viscoelasticity. Both expressions represent the nonequilibrium thermodynamical imbalance due to the load and chemical potential effects, generating viscoelasticity and poroelasticity response (Hu and Suo, 2012).

$$\left[\frac{\partial A}{\partial \epsilon_{ij}} - \frac{(\mu - \mu_0)}{\Omega}\delta_{ij} - \sigma_{ij}\right]\delta\epsilon_{ij} + \frac{\partial A}{\partial \hat{\epsilon}_{ij}}\delta\hat{\epsilon}_{ij} \leq 0 \qquad (12)$$

$$\frac{\partial A}{\partial \epsilon_{ij}} = \frac{(\mu - \mu_0)}{\Omega}\delta_{ij} + \sigma_{ij} \qquad (13)$$

$$\frac{\partial A}{\partial \hat{\epsilon}_{ij}}\delta\hat{\epsilon}_{ij} \leq 0 \qquad (14)$$

5.2. Finite deformation with a single solvent diffusion

5.2.1. The deformation gradient and the nominal stress

Also knows as deformation gradient tensor $\bar{\bar{F}}$. In general, the deformation gradient can break down by the product of elastic $\bar{\bar{F}}^e$ and swelling $\bar{\bar{F}}^s$ elements (Chester and Anand, 2010; Chester and Anand 2011; Chester, 2012). The $\bar{\bar{F}}^s(\boldsymbol{X})$ denote the swelling and local distortion of the polymeric network due to the absorption of fluid molecules inside a structural space $\boldsymbol{X}$.

The $\bar{\bar{F}}^e(\boldsymbol{X})$ correspond to mechanical elastic distortion due to the subsequent stretch and rotation of the polymeric network at structural space $\boldsymbol{X}$. Even the elastic distortion approximates a spontaneous process regarding a significant time-span situation like it is the swelling. Hence the elastic distortion has approximated a value of one. Also, the equilibrium thermodynamic process considers the current deformation state more important than the initial state (Hong et al., 2008).

$$\bar{\bar{F}} = \bar{\bar{F}}^e\bar{\bar{F}}^s \approx \bar{\bar{F}}^s \qquad (15)$$

As a result, the polymeric hydrophilic network allows entry to the system of a large quantity of solvent and other solute species. This process configures an external stimulus to the system that undergoes deformation from the reference (initial) to the current state, as shown in the Figure 5. The deformation gradient or the deformation gradient tensor can define as the present chance process to suffer the system x_i concerning a reference state X_K.

$$F_{iK}(\boldsymbol{X}, t) = \frac{\partial x_i(\boldsymbol{X}, t)}{\partial X_K} = \bar{\bar{F}} \qquad (16)$$

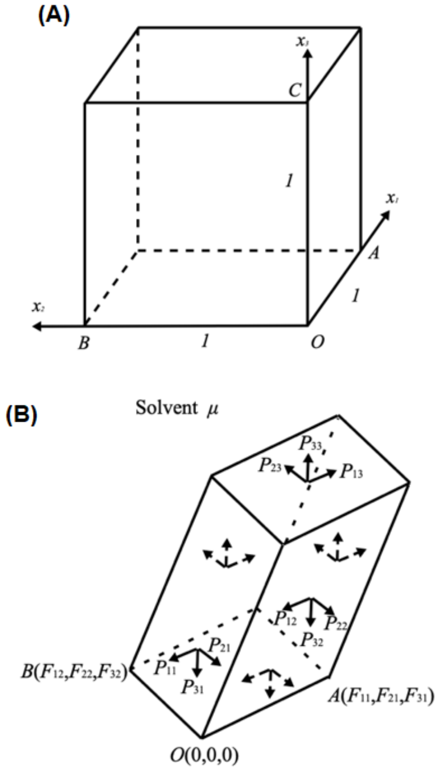

Figure 5. (a) Reference state (initial state) (b)The current state. The cubic polymeric network is in equilibrium with applied forces and the environment with a value of chemical potential, μ . The applied force act on the cube's six faces agrees with the nominal stress definition, P_{iK}. The components of the three vectors define the deformation gradient, F_{iK} (adapted from Cai and Suo, 2012; Hu and Suo, 2012).

The external work done on the hydrogel is related to the variation in the total energy concerning the deformation suffered by the system. The nominal stress P_{iK}, also known as the first Piola-Kirchoff stress tensor, expresses the instantaneous change in the system energy by changing the deformation gradient concerning to a reference state (Liu et al., 2015), as shown in the Figure 5.

$$P_{iK} = \frac{\partial A}{\partial F_{iK}} = \bar{\bar{P}} \tag{17}$$

5.2.2. Solvent diffusion constraints

The small molecules inside the hydrogel system undergo many positional changes. Still, it is necessary to specify the solvent molecules' incompressibility and the polymeric chains due to the negligible void space in condensed matter. Consequently, equation (5) shows the approximation for the total volume, and it can rewrite in terms of swelling radio J as seen in equation (18) (Hong et al., 2008).

$$J = \det \bar{\bar{F}} = \frac{V}{V_0} = 1 + \Omega_1\left(c_1 - c_{1_0}\right) \tag{18}$$

The condition of molecular incompressibility is taken into account inside the equilibrium balance by adding Lagrange multiplier Π , a nonhomogeneous field. As a result, the nominal stress and chemical potential are functions of this multiplier, as seen in equations (19) and (20). The H_{iK} is the transpose of the inverse of the deformation gradient $\left(H_{iK} = \bar{\bar{F}}^{-T}\right)$ with the properties $H_{iK}F_{iL} = \delta_{KL}$ and $H_{iK}F_{jK} = \delta_{ij}$ (Hong et al., 2010).

$$\mu_1 = \left(\frac{\partial A}{\partial C_1}\right)_{T,V,n_{j\neq 1}} + \Pi\Omega \tag{19}$$

$$P_{iK} = \left(\frac{\partial A}{\partial F_{iK}}\right) - \Pi H_{iK} J \tag{20}$$

A possible physical interpretation of field Π is the approximation to osmotic pressure $\Pi \approx \pi$. One way to understand this approximation is to make the analogy with a pure solvent permeation through a polymeric membrane since a solution. In this case, the solvent diffuses doing that the solution pressure arrives at the osmotic value. The osmotic pressure is physically imposition solvable as part of initial and boundary value problems (Hong et al., 2008; Cai and Suo, 2012; Li et al., 2012).

5.2.3. The infinitesimal and finite deformation relation

A direct relation between the infinitesimal deformation and finite deformation theories is the connection between the mechanical load and the nominal stress tensor, as seen in equation (21). The first part of the expression represents the elastic stress exercised by stretching the polymeric network, and the second part can be approximate to the osmotic pressure as said above. In the equilibrium, the elastic stress must be equal to the osmotic pressure, or in the same way, it is not applying a mechanical load $\left(\sigma_{ij} = 0\right)$ (Hong et al., 2008; Hong et al., 2010).

$$\sigma_{ij} = \frac{\partial A}{\partial F_{iK}} \frac{F_{jK}}{\det \boldsymbol{F}} - \Pi\delta_{ij} \cong \frac{P_{iK}F_{jK}}{J} - \pi\delta_{ij} \tag{21}$$

5.2.4. Finite deformation inequality

It proposes a similar setup, as shown in Figure 3. The PHGS, the external force represented by hanging weights, and surroundings constituting the composite close thermodynamic system. We consider a dry polymer network and surroundings constituted by a pure liquid solvent in equilibrium with his vapor in the reference state. The value of solvent chemical potential has been set at zero, the thermodynamics state is independent of translation and rotation rigid-body, and the complete process considering isothermal (Hong et al., 2008). The composite exchange energy with the rest of the universe by heat, but not by work nor mass flux. The system's total energy is the sum of the PHGS energy, the hanging weights' potential energy, and the energy of the surrounding.

If applied on an isothermal composite system, the first and second law of thermodynamics, the two expressions are combined, and collapse in a single dissipation imbalance that expresses the Helmholtz energy decreases (Anand and Govindjee, 2020). Here, the Helmholtz free energy change of the hydrogel volume in a current state concerning the reference state is δA. The current state is associate with a slight change in the deformation gradient δF_{iK} due to applied force in the direction i on the face whose normal vector is in the direction K. Thus, the potential energy changes associated with the hanging weights are the product of the nominal stress and the tiny change in the deformation gradient $-P_{iK}\delta F_{iK}$. The molecules flux from the surroundings to the inside or vice versa of the hydrogel is $-\mu\delta C$, as represented in Figure 5 (Hu and Suo, 2012).

$$\delta A - P_{iK}\delta F_{iK} - \mu\delta C \leq 0 \tag{22}$$

In the imbalance, the equality is related to reversible changes undergoing by the composite near to equilibrium state, and the inequality is associated with irreversible changes suffering by composite out of equilibrium. As commonly in thermodynamics, the inequality expresses the time direction but not the processing time extends (Noll et al., 1974).

5.2.5. The Helmholtz free energy of the system

According to the *Flory-Rehner* theory (Flory and Rehner, 1943), for most types of crosslinking hydrogels, it is valid to assume that the total Helmholtz free energy of system A can be approximate by the sum of the Helmholtz free energy of elastic network stretch A^{el} plus the Helmholtz free energy of mixing A^{mix}. The A^{el} is associated with the crosslinking density, and it is a function of deformation gradient $A^{el} = A^{el}(\bar{\bar{F}})$. The A^{mix} is related to the interactions between the polymer network and the solvent molecules, and it is a function of solvent concentration $A^{mix} = A^{mix}(C_1)$ (Cai and Suo, 2012). However, it is necessary to be careful using this approximation when the polymer used contains a folded domain that cannot unfold after suffering stress. The solvent interactions with the unfolded domains are very different that folded domains (Dušek et al., 2003).

$$A = A^{el}(\bar{\bar{F}}) + A^{mix}(c) + \textstyle\sum_{r\neq 1} A^r \tag{23}$$

The Helmholtz free energy of elastic stretch can be associated with Gaussian statistical theories or non-Gaussian approaches (Arruda and Boyce, 1993). The most usual rubber hyperelasticity model is the Flory description, based on Gaussian statistical as seen in the equation (24) (Liu et al., 2015). Here the N is the number of effective chains in the network, k is the Boltzmann constant, and T the temperature. The product of NkT can be approximate to the elastic modulus of the network G (Huggins, 1941). The scheme shown in Figure 4 can adapt the model to introduce the two-elastic modulus G_1 and G_2 shown in equation (25). The subscript D is equivalent to the referent state in the dry polymer chains (Caccavo and Lamberti, 2017).

An explicit molecular model for the Helmholtz free energy mixing of crosslinking polymer plus solvent does not exist yet. Nevertheless, it is usually assumed that the Helmholtz free energy of mixing in the PHGS has similar functionality to linear polymer plus solvent, namely polymer solution. The Flory-Huggins theory can describe ideal elastomeric gel's behavior, which can approximate the Helmholtz free energy of mixing contributions for solvent-polymer interactions. Here R is the ideal gas constant and c_{1_D} is the water concentration concerning the dry state. The Flory interaction parameter for the isothermal system takes constant values between $0 < \chi_{12} < 1.2$. For temperature-sensitive hydrogels, χ_{12} is a function of temperature and polymer concentration (Huggins, 1941) (see Table 4). Thus

$$A^{el}(\bar{\bar{F}}) = \tfrac{1}{2}\, NkT\left[\mathrm{tr}\left(\bar{\bar{F}}^T\bar{\bar{F}}\right) - 3 - 2\ln\left(\det\bar{\bar{F}}\right)\right] \tag{24}$$

$$A_D^{el}(\bar{\bar{F}}) = \tfrac{G_1}{2}\left[\bar{\bar{F}}_D : \bar{\bar{F}}_D - 3 - 2\ln\left(\det\bar{\bar{F}}_D\right)\right] + \tfrac{G_2}{2}\left[\bar{\bar{F}}_D\left(\bar{\bar{F}}^{visc}\right)^{-1} : \bar{\bar{F}}_D\left(\bar{\bar{F}}^{visc}\right)^{-1} - 3 - 2\ln\left(\det\left(\bar{\bar{F}}_D\left(\bar{\bar{F}}^{visc}\right)^{-1}\right)\right)\right] \tag{25}$$

$$A_D^{mix}(c_1) = RT\left[c_{1_D}\ln\left(\frac{\Omega_1 c_{1D}}{1+\Omega_1 c_{1D}}\right) + \frac{c_{1D}\chi_{12}}{1+\Omega_1 c_{1D}}\right] \tag{26}$$

Table 4. The Helmholtz free energy contribution A^r associate to specific polymeric types of hydrogels (Liu et al., 2015).

PHGS type associated	Model related to specific A^r	Extra-terms involved / References
Polyelectrolytic PHGS	$A^{ion} = kT\sum_{r\neq 1} c_r\left[\ln\left(\frac{c_r}{\Omega_1 c_1 c_{r_0}}\right) - 1\right]$	c_r concentration of the *r* ions (Ricka and Tanaka, 1984; Brannon-Peppas and Peppas, 1991; Hong, et all., 2010; Marcombe, et all., 2010; Yan, et all., 2014)
Unequal distribution of the charge	$A^{pol} = \frac{1}{2\epsilon}\frac{F_{iK}F_{iL}}{\det\bar{\bar{F}}}\widetilde{D}_K\widetilde{D}_L$	ϵ permittivity of the hydrogel. $\widetilde{D}_i$ nominal electrical displacement (Hong, et all., 2010; Yan, et all., 2014)
Dissociation of groups that have weak acid residues AH	$AH \leftrightarrow A^- + H^+$ $A^{dis} = kT\left[c_{A^-}\ln\left(\frac{c_{A^-}}{c_{A^-}+c_{AH}}\right) + c_{AH}\ln\left(\frac{c_{AH}}{c_{A^-}+c_{AH}}\right)\right] + \Delta H^{dis}c_{A^-}$	ΔH^{dis} enthalpy change due to acid dissociates. (Ricka and Tanaka, 1984; Marcombe, et all., 2010)
Photo-thermal hydrogel contained nanoparticles	$X + \hbar f \rightarrow Y,\ \ Y \rightarrow X + heat$ $A^{pho} = N^P\left[\hbar f + kT\ln\left(\frac{N^P}{N^{g,0}}\right)\right]$	f light frequency. $\hbar$ Planck's constant. N^P number of photo-chemical reactions. $N^{g,0}$ affinity associates with a single photo-chemical reaction. (Parson, 1978)
PHGS ingrained with sensible particles that have linear magnetic properties PHGS that experience a phase transition	$A^{mag} = \frac{1}{2\mu^B}\mathbf{B}\cdot\mathbf{B}$ $A^{phase} = \frac{1}{\Omega_1}\left[\frac{1}{2}A_1(T-T_*)\eta^2 + \frac{1}{4}A_2\eta^4 + \frac{1}{6}A_3\eta^6\right]$	μ^B magnetic permeability. $\mathbf{B}$ magnetic induction. (Han, et all., 2011) A_1, A_2 and A_3, constant coefficients. T_* transition temperature. η nematic order parameter. (Drozdov, 2014; Drozdov, 2015)

5.2.6. The indetermination from the dry state

The presence of an indetermination in the Helmholtz free energy of mixing $\left(A_D^{mix} = -\infty\right)$ when the reference state is the dry polymer $\left(c_{1_D} = 0\right)$ can be overcome if another reference state *0* is adopted. So, it is necessary to change of reference frame and use the definition of volumetric deformation for the new initial state $\left(J_0 = \det \bar{\bar{F}}_0\right)$. $\bar{\bar{F}}_0$ is the deformation gradient for the new reference state, and $c_1$is the current solvent concentration.

The equation (27) expresses the sum of the $A^{el}$and A^{mix} concerning the new reference state (Caccavo and Lamberti, 2017).

$$\left(\bar{\bar{F}}, c_1, \bar{\bar{F}}^{visc}\right) = \frac{1}{J_0}\left\{\frac{G_1}{2}\left[\bar{\bar{F}}_0\bar{\bar{F}}{:}\,\bar{\bar{F}}_0\bar{\bar{F}} - 3 - 2\ln\left(\det \bar{\bar{F}}_0\bar{\bar{F}}\right)\right] + \frac{G_2}{2}\left[\bar{\bar{F}}_0\bar{\bar{F}}\left(\bar{\bar{F}}^{visc}\right)^{-1}{:}\,\bar{\bar{F}}_0\bar{\bar{F}}\left(\bar{\bar{F}}^{visc}\right)^{-1} - 3 - 2\ln\left(\det\left(\bar{\bar{F}}_0\bar{\bar{F}}\left(\bar{\bar{F}}^{visc}\right)^{-1}\right)\right)\right] + RT\left[J_0 c_1 \ln\left(\frac{J_0\Omega_1 c_1}{1+J_0\Omega_1 c_1}\right) + \frac{J_0 c_1 \chi_{12}}{1+J_0\Omega_1 c_1}\right]\right\} \qquad (27)$$

5.2.7. The constitutive equations

The inequality (22) can be generalized in its tensor form, with the time like an explicit independent variable, as shown in equation (28) (Holzapfel, 2002; Gurtin et al., 2010). The Helmholtz free energy change is affected by the conventional power expended on the structure $\left(\bar{\bar{P}}{:}\left(\dot{\bar{\bar{F}}}\right)\right)$ and to the energy transported into the hydrogel by the solvent diffusion $\left(-\mu_1\dot{c}_1 + \bar{h}_1\cdot\bar{\nabla}\mu_1\right)$. The deformation gradient and solvent concentration variation concerning to the time is represented as $\left(\dot{\bar{\bar{F}}}\right) = \frac{\partial \bar{\bar{F}}}{\partial t}$ and $\dot{c}_1 = \frac{\partial c_1}{\partial t}$.

$$\frac{\partial A}{\partial t} - \bar{\bar{P}}{:}\left(\dot{\bar{\bar{F}}}\right) - \mu_1\dot{c}_1 + \bar{h}_1\cdot\bar{\nabla}\mu_1 \leq 0 \qquad (28)$$

It requires the continuity equation, or the mass balance for the solvent, that relates the derivate of the solvent concentration concerning time with the gradient of the solvent molar flux $\bar{h}_1$,

$$\frac{\partial c_1}{\partial t} = -\bar{\nabla}\cdot\overline{h_1} \qquad (29)$$

Also, linear momentum balance is necessary, which has been written using the quasistatic approach because it considers that the diffusional process's time scale is much longer than the one associated with inertia, so that the inertia terms can be disregarded.

$$\bar{\nabla}\cdot\bar{\bar{P}} = \bar{0} \qquad (30)$$

Additionally, it is necessary to consider the swelling radio related to the solvent diffusion constraints shown in equation (18) (Caccavo and Lamberti, 2017). It is recommended the use the relaxed Helmholtz free energy version because it includes the constraints of solvent diffusion and is a function of osmotic pressure as another variable.

$$A_R\left(\bar{\bar{F}}, c_1, \bar{\bar{F}}^{visc}, \pi\right) = A\left(\bar{\bar{F}}, c_1, \bar{\bar{F}}^{visc}\right) - \pi\left\{J - \left[1 + \Omega_1\left(c_1 - c_{1_0}\right)\right]\right\} \qquad (31)$$

Now, if the relaxed Helmholtz free energy is differentiated concerning the time, two-aspect are recognized: (i) the satisfaction of the definitions for the nominal stress tensor, equation (19), and the chemical potential, equation (20), which include the solvent diffusion constraints. Thus, we can say that these equations are constitutive for $\bar{\bar{P}}$ and μ_1, and conform the equality conditions into the imbalance; (ii) this differentiation process demonstrates that $\left(\frac{\partial A_R}{\partial \bar{\bar{F}}} = \frac{\partial A}{\partial \bar{\bar{F}}}\right)$. Therefore, it required two additional constitutive equations to satisfice the imbalance in any situation, punctually the inequality. These expressions indicate the kinetic laws for the solvent flux and the dashpot deformation, as it is shown in the equation (32) and (33). The kinetics equations have to be the form as presents in equations (34) and (35).

$$\bar{h}_1\cdot\bar{\nabla}\mu_1 \leq 0 \qquad (32)$$

$$\frac{\partial A_R}{\partial \bar{\bar{F}}^{visc}}\frac{\partial \bar{\bar{F}}^{visc}}{\partial t} \leq 0 \qquad (33)$$

$$\bar{h}_1 = -\bar{\bar{D}}_1\bar{\nabla}\mu_1 \qquad (34)$$

$$\frac{\partial \bar{\bar{F}}^{visc}}{\partial t} = -\frac{1}{\eta}\frac{\partial A_R}{\partial \bar{\bar{F}}^{visc}} = -\frac{1}{\eta}\frac{\partial A}{\partial \bar{\bar{F}}^{visc}} \qquad (35)$$

The η is the dashpot's dynamic viscosity and represents the viscous dissipation associated with the G_2 and the relaxation time $\left(\tau_R = \eta/G_2\right)$ (Holzapfel, 2002). The $\bar{\bar{D}}_1$ is the mobility tensor, described by the equation (36), that is a function of diffusivity of the solvent into the hydrogel structure D_{1s}.

$$\bar{\bar{D}}_1 = J\frac{D_{1s}}{\Omega_1 RT}\;\bar{\bar{F}}^{-T}\bar{\bar{F}}^{-1} \qquad (36)$$

6. Poroviscoelasticity approach with a single solvent diffusion

The scheme showing in Figures 6a and 6b represent the linear poroviscoelasticity from a Biot theory (Biot, 1956) and the theory of the nonlinear field for hydrogels (Hu and Suo, 2012;

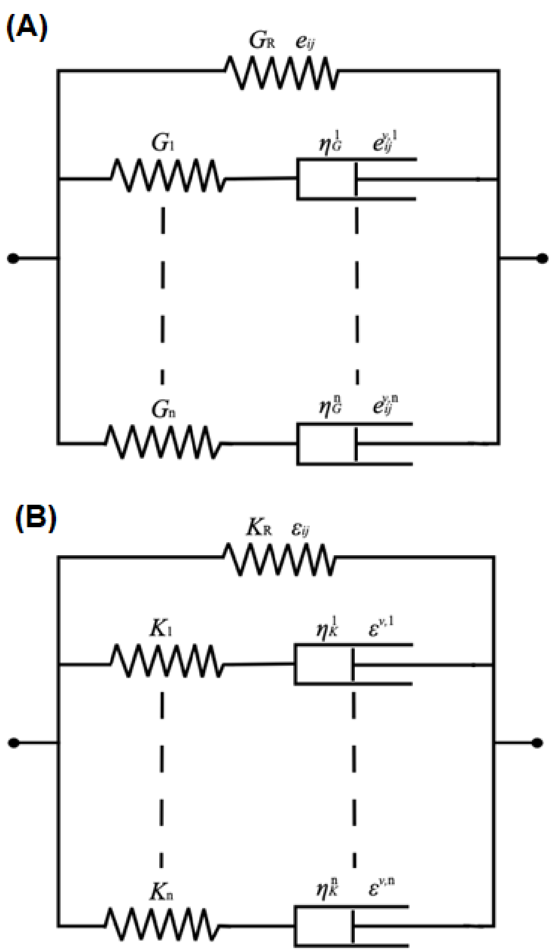

Figure 6. Rheological representation for the deviatoric and volumetric components of poroviscoelastic gel, in the poroviscoelastic approach: (a) deviatoric component; (b) volumetric component (adapted from Wang et al., 2014).

Wang and Hong, 2012). The linear theory assumes the system's strain like a function displacement field time-dependent $u_i = u_i(x_1, x_2, x_3, t)$, how it is shown in the equation (37).

$$\epsilon_{ij} = \frac{1}{2}\left(\frac{\partial u_i}{\partial x_j} + \frac{\partial u_j}{\partial x_i}\right) \qquad (37)$$

The components of the strain tensor ϵ_{ij} are the volumetric dilatation ϵ_{kk} and its deviatoric component e_{ij}, as seen in equations (38) and (39). The components of the strain tensor σ_{ij} are the hydrostatic σ and its deviatoric s_{ij}, as seen in equations (40) and (41).

$$\epsilon = \epsilon_{kk} \qquad (38)$$

$$e_{ij} = \epsilon_{ij} - \frac{1}{3}\epsilon\delta_{ij} \qquad (39)$$

$$\sigma = \frac{1}{3}\sigma_{kk} \qquad (40)$$

$$s_{ij} = \sigma_{ij} - \sigma\delta_{ij} \qquad (41)$$

This approach uses the same definitions for the continuity eq. (29), the chemical potential eq. (7), and the solvent diffusion constraints for the component ϵ_{kk} shown in the eq. (18). The current Helmholtz free energy is a function of the strain tensor, the deviatoric component, the solvent concentration, and the internal variables that characterized the viscoelastic properties of the system $\left(\epsilon^{v,n}, e_{ij}^{v,n}\right)$, as seen in equation (42). The change Helmholtz free energy concerning internal variables have the forms shown in equations (43) and (44). Figure (6a) represents the viscosity of the *n*-th volumetric viscous *i*-component. Figure (6b) represents the η_G^n as the viscosity of *n*-th deviatoric viscous *i*-component.

$$A = A\left(\epsilon, e_{ij}, C, \epsilon^{v,1}, \dots, \epsilon^{v,n}, e_{ij}^{v,1}, \dots, e_{ij}^{v,n}\right) \qquad (42)$$

$$\dot{\epsilon}^{v,n} = -\frac{1}{\eta_K^n}\frac{\partial A}{\partial \epsilon^{v,n}} \qquad (43)$$

$$\dot{e}_{ij}^{v,n} = -\frac{1}{2\eta_G^n}\frac{\partial A}{\partial e_{ij}^{v,n}} \qquad (44)$$

The change of the Helmholtz free energy concerning the strain tensors is shown in equation (45), and its change concerning the deviatory component is shown in equation (46).

$$\sigma = \frac{\partial A}{\partial \epsilon} \qquad (45)$$

$$s_{ij} = \frac{\partial A}{\partial e_{ij}} \qquad (46)$$

The Helmholtz free energy function for poroviscoelastic gel has been proposed according to the scheme shown in Figures 6a and 6b. Here, the G_R is the relaxed shear modulus, the G_n is the shear modulus of the *n*-th shear component, the K_R is the relaxed bulk modulus, and the K_n is the bulk modulus of the *n*-th bulk component.

$$A = G_R {e_{ij}}^2 + \frac{1}{2}K_R\epsilon^2 + \sum_n G_n\left(e_{ij} - e_{ij}^{v,n}\right)^2 + \frac{1}{2}\sum_n K_n\left(\epsilon - \epsilon^{v,n}\right)^2 + \pi\left[\Omega_1\left(c_1 - c_{1_0}\right) - \epsilon\right] \qquad (47)$$

It considers the above thermodynamical framework, the linear poroviscoelasticity considerations, and the kinetic expressions. In that case, it is possible to express the stress tensor in terms of the Prony series, which is a function of the PHGS mechanical properties, the time, and the characteristic time τ_n (Wang et al., 2014).

$$\sigma_{ij} = 2G_U\left\{1 - \sum_n g_n\left[1 - \exp\left(-\frac{t}{\tau_n}\right)\right]\right\}\left(\epsilon_{ij} + \frac{\nu}{1-2\nu}\epsilon_{kk}\delta_{ij}\right) - \frac{\mu-\mu_0}{\Omega}\delta_{ij} \qquad (48)$$

The G_U is the unrelaxed shear modulus, as seen in equation (49). The K_U is the unrelaxed bulk modulus, as seen in equation (50). Moreover, the *n*-th viscous component's characteristic time τ_n, as seen in equation (51). The *n*-th term of the Prony series g_n is a relation between the unrelaxed shear modulus and the shear modulus of the *n*-th shear component, as seen in equation (52). The ν is the effective Poisson's ratio of the PHGS (Hu and Suo, 2012).

$$G_U = G_R + \sum_n G_n \qquad (49)$$

$$K_U = K_R + \sum_n K_n \qquad (50)$$

$$\tau_n = \tau_G^n = \tau_K^n \qquad (51)$$

$$g_n = \frac{G_n}{G_U} \qquad (52)$$

Darcy's law describes the flux of the solvent (Yoon et al., 2010). A modified continuity equation is the outcome of using this flux description and the model described in equation (48), as seen in equation (53). The D_e is the effective diffusivity which is a function of the dynamic viscosity of PHGS and the experimental permeability of the structure κ (Hui et al., 2006), as seen in equation (54).

$$\frac{\partial c_1}{\partial t} = D_e \bar{\nabla}^2 \bar{h}_1 \qquad (53)$$

$$D_e = G_U\left\{1 - \sum_n g_n\left[1 - \exp\left(-\frac{t}{\tau_n}\right)\right]\right\}\frac{2(1-\nu)\kappa}{(1-2\nu)\eta} \qquad (54)$$

7. Multicomponent mass transfer

So far, the developed approaches and the constitutive equations have considered the single solvent diffusion through the PHGS structure. However, other solute species' presence affects the swelling process, and it is relevant when it is interest species like a drug-delivering or advance separation process. Thus, the real chemical potential must consider the simultaneity of the mechanical effects and the multicomponent interaction in the diffusive and swelling process (Caccavo et al., 2020). The "fully coupled models" describe complete hydrogel systems changes as a function of time and space, linked the multicomponent mass transfer process with the mechanic effects and vice-versa (Caccavo, 2019).

7.1. Mass transfer regimen

The mass transport regimen in hydrogel systems characterizes the mechanism and structure influence that governs the solvent and solute species absorption/desorption. The know regimens are the Fickian regimen driven by a gradient concentration and the non-Fickian regimen, which is a deviation of the first regimen due to polymer network movements. The diffusion Deborah number $N_{De.D}$ is one way to establish the regimen that government the phenomena, where τ is the characteristic stress-relaxation time of the polymer-solvent system and is τ_D the characteristic time for the solvent diffusion in the polymer network. The determination of the stress – relaxation time is making by the calculus of the shear relaxation modulus integrals $G(t)$ through the entire relaxation time finite range t. The solvent diffusion time calculation does by the ratio of the second power of the characteristic diffusion path length for the solvent L_{Ch}^2 and the solvent's diffusion in the swollen polymer network $D_{1.s}$ (Vrentas et al., 1975; Vrentas and Duda, 1977; Caccavo, 2019).

$$N_{De.D} = \frac{\tau}{\tau_D} = \frac{\left(\dfrac{\int_0^\infty sG(s)ds}{\int_0^\infty G(s)ds}\right)}{\dfrac{L_{Ch}^2}{D_{1.s}}} \qquad (55)$$

The change in the solvent concentration during the swelling process dictates the way to calculate the Deborah number. Suppose the solvent experiences a limited concentration change. In that case, the estimate of $N_{De.D}$ is done by the average values for each characteristic time used, and a unique value describes the complete process. Now, suppose the change in the solvent concentration is drastic. In that case, the calculation of $N_{De.D}$ is done at the initial and the final stage of the process, and their order of magnitude will characterize the system's behavior. The Deborah's number magnitude and its phenomenological implications as show in the Table 5.

7.2. Finite deformation with a multicomponent mass diffusion

7.2.1. Constitutive couple models

The definition of osmotic pressure needs to be modified to describe a complete system that arises by interacting with the solvent, the polymer, and the other solute species. Here, the π is a function of the absolute temperature T, the constant gas R, the *i-th* species concentration within the PHGS c_i, and the *i-th* species concentration in the external medium or bulk c_i^{ext}. The subscript is 1 to solvent, 2 to polymer, and $i = 3 \ldots N$ for the other solute species.

$$\pi = RT\sum_{\substack{i=1 \\ i\neq 2}}^{N}\left(c_i - c_i^{ext}\right) \qquad (56)$$

The moment balance remains the same as seen in equation (30).

Table 5. The Deborah's number magnitude and its phenomenological implications (Davidson and Peppas, 1986).

Deborah's number magnitude	Time relations	Indications and remarks	Description of diffusion phenomena and its coefficient
$\boldsymbol{N_{De.D}} \gg 1$	$\tau \gg \tau_D$	The large values of Deborah's number specify that the characteristic relaxation time is much larger than the characteristic time for solvent diffusion. The network structure does not change in the diffusion process, and the polymer remains in a glassy state	The diffusion phenomena are describing by a conventional Fick law. The diffusion coefficients are constants and independents of solvent and polymer concentration.
$\boldsymbol{N_{De.D}} \ll 1$	$\tau \ll \tau_D$	The small values of Deborah's number show that the characteristic relaxation time is much faster than the characteristic time for solvent diffusion. The phenomena are considered a diffusion through a vicious media conformed by a swollen and rubbery hydrogel.	The diffusion phenomena are describing by a conventional Fick law. In this case, the diffusion coefficients are a stronger function of solvent and polymer concentration.
$\boldsymbol{N_{De.D}} \sim 1$	$\tau \sim \tau_D$	The intermediated values of Deborah's number denote that the characteristic relaxation time and the characteristic time for solvent diffusion are of the same order of magnitude, and both phenomena take place on the same time scale. The phenomena are considered a diffusion in a transition region where the polymer experiences its glass-rubber change. The mixture has a viscoelastic nature.	The diffusion phenomena are describing by a non-Fickian model, and the diffusion is anomalous transport.

The continuity equation writes in general terms concerning to Lagrange reference frame for the species *i-th* concentration and the molar diffusive flux $\mathbf{J}_i^*$. This equation is truthy for any diffusive system without any simplification (Caccavo, 2019).

$$\frac{\partial c_i}{\partial t} = -\bar{\nabla} \cdot \mathbf{J}_i^* \qquad \forall i \neq 2 \qquad (57)$$

The swelling radio related to the volume constraints, Equation (18), needs to be modified to include the other solute species as seen in equation (58). Here, J is the Jacobian of the deformation gradient $\bar{\bar{F}}$ or the volumetric constraint, the Ω_i is the i-th species' molecule volume, and c_{i_0} is the initial concentration of the *i-th* species. The summation inside the equation does not consider the polymer species ($i = 2$) because the solute and the solutes are the only diffusive species.

$$J = 1 + \sum_{\substack{i=1 \\ i \neq 2}}^{N} \Omega_i \left(c_i - c_{i_0}\right) \qquad (58)$$

The inequality equation in its tensor form derives from nonequilibrium thermodynamics, Equation (28), requirements to be modified to include the other solute species as seen in equation (59). The relaxed version of the Helmholtz free energy uses to impose the above volumetric constraint, as seen in equation (60). Again, the Helmholtz free energy A is calculated using the sum of elastic contribution, the mixing and others possible contributions regarding to the equation (23) and agree to the Table 4.

$$\frac{\partial A_R}{\partial t} - \bar{\bar{P}}\colon\left(\dot{\bar{\bar{F}}}\right) - \sum_{\substack{i=1 \\ i \neq 2}}^{N} \left(\mu_i \dot{c}_i + \bar{h}_i \cdot \bar{\nabla} \mu_i\right) \leq 0 \qquad (59)$$

$$A_R = A - \pi \left(J - 1 - \sum_{\substack{i=1 \\ i \neq 2}}^{N} \Omega_i (c_i - c_{i0}) \right) \qquad (60)$$

The function of Helmholtz free energy as $A = A\left(\bar{\bar{F}}, \bar{\bar{F}}^{visc}, c_1\right)$ must consider the energy contribution of other solute species, how it presents in equation (61). In this expression, the standard linear solid model describes the viscoelastic term again. The mixing contribution considers the enthalpy contribution by the interaction between the solvent and the polymer, and the other solute species have only an entropy energetic input.

To avoid indetermination to the dry polymer state ($c_{1_D} = 0$), the tensor deformation $\bar{\bar{F}}_0$ and its Jacobian J_0 are measures in concerning a different state, similar to equation (27). The φ_i is the volumetric fraction of the ($i = 1 \ldots N$) component that considers the additive volume simplification (Eq. (4)).

$$A\left(\bar{\bar{F}}, \bar{\bar{F}}^{visc}, c_1\right) = \frac{1}{J_0} \left\{ \frac{G_1}{2} \left[\bar{\bar{F}}_0 \bar{\bar{F}} \colon \bar{\bar{F}}_0 \bar{\bar{F}} - 3 - 2 \ln(J_0 J)\right] + \frac{G_2}{2} \left[\bar{\bar{F}}_0 \bar{\bar{F}} \left(\bar{\bar{F}}^{visc}\right)^{-1} \colon \bar{\bar{F}}_0 \bar{\bar{F}} \left(\bar{\bar{F}}^{visc}\right)^{-1} - 3 - 2 \ln\left(J_0 J \det\left(\bar{\bar{F}}^{visc}\right)^{-1}\right)\right] \right.$$
$$\left. + RT \left[J_0 c_1 \ln(\varphi_1) + \sum_{\substack{i=1 \\ i \neq 2}}^{N} J_0 c_i \ln(\varphi_i) + J_0 c_1 \chi_{12} \varphi_2 \right] \right\} \qquad (61)$$

According to the rheological model shown in Figure 4, the G_1 is the shear modulus parameter of the relaxed system associate with the elastic response, and the G_2 is the shear modulus parameter due to the viscoelastic response described with a Maxwell element, a function of viscous deformation tensor $\bar{\bar{F}}^{visc}$. Again, the η is the viscosity of the dashpot $\left(\tau_R = \eta / G_2\right)$.

Using the adequate expression for the Helmholtz free energy and its derivation concerning the time, the imbalance equation (59) must satisfice the Helmholtz free energy change for the tensor deformation, Equation (20). Further, it needs to be satisfied the Helmholtz free energy change concerning the concentration of *i-th* species, as seen in equation (62).

$$\mu_i = \left(\frac{\partial A}{\partial C_i}\right)_{T,V,n_{j\neq i}} + \pi\Omega_i \qquad (62)$$

The Helmholtz free energy imbalance, equation (59), gives conditions on the kinetic of the molar flux to all diffusional species $(i \neq 2)$ and the viscous relaxation of the structure, represented with the inequality (63) and (64) (Caccavo et al., 2018).

$$\bar{h}_i \cdot \bar{\nabla}\mu_i \leq 0 \qquad (63)$$

$$\frac{\partial A_R}{\partial \bar{\bar{F}}^{visc}} \frac{\partial \bar{\bar{F}}^{visc}}{\partial t} \leq 0 \qquad (64)$$

Complete satisfaction of the imbalance, equation (59), needs a kinetic law for a viscous behavior. Thus, the dashpot deformation model, a constitutive equation, remains the same, as shown in equation (35).

7.3. Molar flux models

7.3.1. Fickian diffusion

A kinetic law model for a molar flux is obtained from the imbalance (Eq. (59)). The model describes the flux due to concentration gradient disregarding any presence of relevant body forces, such as electrostatic field (Caccavo, 2019; Caccavo et al., 2020).

$$\bar{h}_i = -\bar{\bar{D}}_i \bar{\nabla}\mu_i \qquad \forall i \neq 2 \qquad (65)$$

7.3.2. Non-Fickian diffusion

An approximation from stress-assisted diffusion theory considers that the molar flux is a sum of a concentration and stress driving force (Aifantis, 1980; Siepmann and Siepmann, 2012; Ferreira et al., 2018).

$$\bar{h}_i = -D_{is}\bar{\nabla}c_i + \bar{\bar{D}}_i \bar{\nabla}\left(\operatorname{tr}\left(\bar{\bar{\mathrm{P}}}\right)\right) \qquad \forall i \neq 2 \qquad (66)$$

7.3.3. Mobility tensor

The $\bar{\bar{D}}_i$ is the positively defined mobility term that is a tensor for isotropic materials. It related the species' movement into the structure and affected the swelling velocity, which can relate to the diffusivity or permeability. A common assumption considers that the diffusivity always remains isotropic during any process, and it is a function of constant binary diffusivity of the solute i into PHGS structure D_{is} and solvent concentration c_1(Chester and Anand, 2010; Lucantonio et al., 2013).

$$\bar{\bar{D}}_i = D_{is} \frac{c_1}{RT} \bar{\bar{F}}^{-T} \bar{\bar{F}}^{-1} \qquad \forall i \neq 2 \qquad (67)$$

7.3.4. Maxwell-Stefan multicomponent approach

The Maxwell-Stefan formulation (MS) advantages over the Fick formulation have been recognized, mainly when the situation implies more than two components. These impossibilities reflect in the non-symmetrical diffusive coefficients $\left(D_{ij} \neq D_{ji}\right)$, its strong concentration reliance, and numerical values depend on the particular choice of system numbering. As a result, the binary system's data have very restricted applicability for predicting molar fluxes in multicomponent systems (Taylor and Krishna, 1993; Krishna and Wesselingh, 1997; Ribeiro et al., 2011).

Usually, the MS equations are written in terms of mass fraction, which is a problem if one of the components is a polymer because its molecular weight is unknown or has a complex distribution (Sanchez and Lacombe, 1978; Kiszka et al., 1988; Barbari and Conforti, 1992). The MS equations write in terms of volume fraction to overcome this situation and helps to use the Flory-Huggins model simultaneously. This expression is simultaneously consistent with the Gibbs – Duhem restriction and Onsager reciprocity relations (Ribeiro et al., 2011).

$$\frac{\varphi_i}{\bar{V}_i RT} \nabla\mu_i = -\sum_{j=1}^{m} \left(\frac{\bar{h}_i \varphi_j}{\mathfrak{D}_{ij}} - \frac{\varphi_i \bar{h}_j \bar{V}_j}{\mathfrak{D}_{ij} \bar{V}_i}\right) \qquad (68)$$

The chemical potential measure is done at constant temperature and pressure $\left(\nabla\mu_i = \nabla_{T,P}\mu_i\right)$. To use the general continuity equation (57) requires a relation between the molar diffusive flux and the molar flux relative to stationary coordinates, where x_i is the molar fraction, as seen in equation (69). The $\bar{V}_i$ is the partial molar volume, as shown in equation (70). The D_{ij} is the modified MS diffusion coefficient, where $Đ_{ij}$ is the MS diffusion as seen in equation (71) (Taylor and Krishna, 1993; Ribeiro et al., 2011).

$$\bar{h}_i = \mathbf{J}_i^* + x_i \sum_{i=1}^{m} \bar{h}_i \qquad (69)$$

$$\overline{\mathrm{V}}_{\mathrm{i}} = \left(\frac{\partial \mathrm{V}}{\partial \mathrm{n_i}}\right)_{\mathrm{T,V,n_{j\neq i}}} \qquad (70)$$

$$\mathfrak{D}_{ij} = \frac{\text{Đ}_{ij}\bar{V}_j}{\sum_{k=1}^{m} x_k \bar{V}_k} \qquad (71)$$

The MS diffusivities Đ_{ij} calculation is possible in polymeric multicomponent mixtures from the Fick diffusivities (Liu et al., 2011; Kubaczka, 2014). Some hydrogel system practical applications used this approach (Fornasiero et al., 2005; Fornasiero et al., 2006; Fornasiero et al., 2008).

7.4. Fick diffusivity coefficients for the PHGSs

The hydrodynamic theory predicts the solute diffusivity ($i = 3 \ldots N$) in a pure liquid solvent D_{i1} through the Stokes-Einstein equation. Here, the k_b is the Boltzmann constant, and the r_i is the solute hydrodynamic radius (Cukier, 1984).

$$D_{i1} = \frac{k_b T}{6\pi\eta r_i} \qquad (72)$$

Generally, the models to compute the solute's diffusivity into hydrogel structure D_{is} have the typical form that uses a multiplication function $f(\xi, \varphi_2, r_i)$, where ξ is the average mesh sizes of the network. This function corrects the pure liquid diffusion of the solute for effect generated by the polymeric network's presence that exerts a sieving impact. Two theories have been using to create a phenomenological function: (i) free volume theory, which adopts a transport via dynamic empty spaces between the molecules (molecular scale) (Cohen and Turnbull, 1959); (ii) obstruction theory, which consider the polymeric network as a barrier for the diffusion of the dilute solute (nanometric and micrometric scale) (Mackie and Meares, 1955).

The likelihood that both phenomena happen $P(FV \cup \xi)$ represents the complete function. However, the probability that the solute will diffuse by two mechanisms simultaneously is zero because the two events are essentially mutually exclusive as they happen at a distinct length scale. Many functional forms exist for the two theories in separate ways (Kapur et al., 1996; Amsden, 1998; Amsden, 1999). Nevertheless, it is possible to express both mechanisms' likelihood by the sum of two individual probabilities, representing the physical possibility of one mechanism being more present than the other, as shown in the equation (73). The compound expression uses the Gaussian error function ($\mathrm{erf}(x)$) and its complementary ($\mathrm{erfc}(x)$) as weight prefactors that are based on a physical theory and do not in empirical observations, as seen in equation (74) (Axpe et al., 2019). This model considers an intermolecular force negligible (Lustig and Peppas, 1988; Hadjiev and Amsden, 2015; Hansing and Netz, 2018).

$$\frac{D_{is}}{D_{i1}} = f(\xi, \varphi_2, r_i) \approx P(FV \cup \xi) = P(FV) + P(\xi) \qquad (73)$$

$$\frac{D_{is}}{D_{i1}} = \left[\mathrm{erf}\left(\frac{r_{FV}}{r_i}\right)\exp\left(-\left(\frac{r_i}{r_{FVW}}\right)^3\left(\frac{\varphi_2}{1-\varphi_2}\right)\right) + \mathrm{erfc}\left(\frac{r_{FV}}{r_i}\right)\exp\left(-\pi\left(\frac{r_i + r_2}{\xi + 2r_2}\right)^2\right)\right] \qquad (74)$$

The r_{FV} is the average radius of the free volume voids comparable with the r_i to determinate the dominate mechanism: ($r_{FV} \sim r_i$) the diffusion via free volume dominates; ($r_{FV} \ll r_i$) the mesh sizes are the limiting factor because the size of solute is as much large as the free volume void. The r_{FVW} is the radius of the water's free volume void as a solvent that is 2.69 Å (Kotera et al., 2005; Hagel et al., 2013). The positron annihilation lifetime spectroscopy (PALS) has been using to determine the free volume radius (Axpe et al., 2014; Giri et al., 2015; García-Arribas et al., 2016). The hydrogel's mesh size is experimental determination, typically using spherical indentation (Offeddu et al., 2018).

5. Conclusions

The poroviscoelasticity as macroscopic dynamic behavior, characteristic of the PHGS, was associated with the microscopic events of viscoelasticity and poroelasticity. The first was related by a conformational event in and between polymers chains, and the second with a diffusion of solutes and solvents through the polymeric network by the action of the differences in the chemical potential. Both behaviors were linked by a characteristic time unique for a pair polymer-solvent. Also, macroscopical physical-chemical properties of PHGS were explained in terms of the chemical or physical crosslinking and by the chemical bonds present between the polymer chains. The equilibrium state of PHGS with the surroundings was shown in terms of the swelling mass ratio, the osmotic pressure, and the energy balance. Then, the infinitesimal and finite deformation approaches could describe the dynamical behavior of the PHGSs concerning the changes in the total Helmholtz free energy of the system due to the actions of the mechanical forces and differences in the chemical potential. The total Helmholtz free energy of the system was calculated as a sum of the individual contributions of the Helmholtz free energy related to specific phenomena, especially to the elastic Helmholtz free energy and the mixing Helmholtz free energy. In the same section, the poroviscoelasticity approach, founded in a discrete rheological model, described the deformation of the PHGSs as a function of macroscopical properties of the system, as the shear modulus, the Poisson ratio, the viscosity of the system, and the experimental permeability. The final section has exposed the multicomponent mass transfer in PHGSs, where a way to know the mass transfer regimen was explained. The finite deformation approach extends to include other chemical species, as solutes and counterions, inside the model structure. The molar flux calculation of the chemical species through the PGHS structure and the diffusional coefficients under the action of the polymeric network was expounded. Thence, the selection of a model is limited for the complexity requirements of the PHGS application. Thus, for example, it is necessary to know when a particular situation needs to include extra definitions of the Helmholtz free energy or where it is crucial the use the multicomponent mass transfer description. Future works are expected, where the equation group conformed by the constitutive equations, and the implicit constraints configure an initial and boundary problem. Dynamic simulations of PHGSs can be done using the models exposed or similar inside the finite element method (FEM), a meshless method, the Monte Carlo technic, or others. Based on experimental data, other future studies are awaited how it is the case of a model for the mixing Helmholtz free energy in the PHGSs that can describe the interaction of the solvent with the polymeric crosslinking network without the simplification of linear polymer (Flory- Huggins model).

⁂

Conflict interest. Authors declare that there is no conflict of interest.

Acknowledgements. Authors thanks to Mindtech s.a.s., Universidad del Valle, Universidad de Córdoba, and Science and Technology Ministry of Colombia for financial support (Postdoctoral fellowships 848-2019 and C.I. 71260).

References

[1] Abasalizadeh, F., Moghaddam, S.V., Alizadeh, E., Akbari, E., Kashani, E., Fazljou, S.M.B., Torbati, M., Akbarzadeh, A. (2020) Alginate-based hydrogels as drug delivery vehicles in cancer treatment and their applications in wound dressing and 3D bioprinting. *Journal of Biology Engineering*. 14, 8. https://doi.org/10.1186/s13036-020-0227-77

[2] Aifantis, E.C. (1980) On the problem of diffusion in solids. *Acta Mechanica*. 37(3–4), 265–296. https://doi.org/10.1007/BF01202949

[3] Amsden, B. (1998) Solute diffusion within hydrogels. Mechanisms and models. *Macromolecules*. 31(23), 8382–8395. https://doi.org/10.1021/ma980765f

[4] Amsden, B. (1999) An Obstruction-Scaling Model for Diffusion in Homogeneous Hydrogels. *Macromolecules*. 32(3), 874–879. https://doi.org/10.1021/ma980922a

[5] An, Y., Solis, F.J., Jiang, H. (2010) A thermodynamic model of physical gels. *Journal of the Mechanics and Physics of Solids*. 58(12), 2083–2099. https://doi.org/10.1016/j.jmps.2010.09.002

[6] Anand, L., Govindjee, S. III – Balance laws. VII – Coupled theories. XI - Finite elasticity. Continuum Mechanics of Solids. *Oxford University Press*. (2020) 67-94, 255-298, 609-636.

[7] Arruda, E.M., Boyce, M.C. (1993) A three-dimensional constitutive model for the large stretch behavior of rubber elastic materials. *Journal of the Mechanics and Physics of Solids*. 41(2), 389–412. https://doi.org/10.1016/0022-5096(93)90013-6

[8] Axpe, E., Chan, D., Offeddu, G.S., Chang, Y., Merida, D., Hernandez, H.L., Appel, E.A. (2019) A Multiscale Model for Solute Diffusion in Hydrogels. *Macromolecules*. 52(18), 6889–6897. https://doi.org/10.1021/acs.macromol.9b00753

[9] Axpe, E., Lopez-Euba, T., Castellanos-Rubio, A., Merida, D., Garcia, J.A., Plaza-Izurieta, L., Fernandez-Jimenez, N., Plazaola, F., Bilbao, J.R. (2014) Detection of atomic scale changes in the free volume void size of three-dimensional colorectal cancer cell culture using positron annihilation lifetime spectroscopy. *PLoS ONE*. 9(1), 1–5. https://doi.org/10.1371/journal.pone.0083838

[10] Barbari, T.A., Conforti, R.M. (1992) The effect of lattice compressibility on the thermodynamics of gas sorption in polymers. *Journal of Polymer Science Part B: Polymer Physics*. 30(11), 1261–1271. https://doi.org/10.1002/polb.1992.090301111

[11] Barbut, S., Foegeding, E.A. (1993) Ca2+-Induced Gelation of Pre-heated Whey Protein Isolate. *Journal of Food Science*. 58(4), 867–871. https://doi.org/10.1111/j.1365-2621.1993.tb09379.x

[12] Bashir, S., Hina, M., Iqbal, J., Rajpar, A.H., Mujtaba, M.A., Alghamdi, N.A., Wageh, S., Ramesh, K., Ramesh, S. (2020) Fundamental Concepts of Hydrogels: Synthesis, Properties, and Their Applications. Polymers. 12(11), 2702. https://doi.org/10.3390/polym12112702

[13] Beebe, D.J., Moore, J.S., Bauer, J.M., Yu, Q., Liu, R.H., Devadoss, C., Jo, B. (2000) Functional hydrogel structures for autonomous flow control inside micro fluidic channels. *Nature*. 404, 588-590. https://doi.org/10.1038/35007047

[14] Berger, J., Reist, M., Mayer, J.M., Felt, O., Gurny, R. (2004) Structure and interactions in chitosan hydrogels formed by complexation or aggregation for biomedical applications. *European Journal of Pharmaceutics and Biopharmaceutics*. 57 (2004) 35-52. https://doi.org/10.1016/S0939-6411(03)00160-7

[15] Biot, M.A. (1956) Theory of deformation of a porous viscoelastic anisotropic solid. *Journal of Applied Physics*. *27*(5), 459–467. https://doi.org/10.1063/1.1722402

[16] Borgogna, M., Skjak-Braek, G., Paoletti, S., Donati, I. (2013) On the Initial Binding of Alginate by Calcium Ions. The Tilted EggBox Hypothesis. *The Journal of Physical Chemistry B*. 117 (24) 7277-7282. https://doi.org/10.1021/jp40307666

[17] Brannon-Peppas, L., Peppas, N.A. (1991) Equilibrium swelling behavior of pH-sensitive hydrogels. *Chemical Engineering Science*. 46, 715-722. https://doi.org/10.1016/0009-2509(91)80177-Z

[18] Bush, B.G., Shapiro, J.M.,DelRio, F.W., Cook, R.F., Oyen, M.L., (2015) Mechanical measurements of heterogeneity and length scale effects in PEG-based hydrogels. *Soft Matter*. 11, 7191. https://10.1039/c5sm01210d

[19] Caccavo, D., Cascone, S., Lamberti, G., Barba, A.A. (2018) Hydrogels: Experimental characterization and mathematical modelling of their mechanical and diffusive behaviour. *Chemical Society Reviews*. 47(7), 2357–2373. https://doi.org/10.1039/c7cs00638a

[20] Caccavo, D., Lamberti, G. (2017) PoroViscoElastic model to describe hydrogels' behavior. *Materials Science and Engineering C*. 76, 102–113. https://doi.org/10.1016/j.msec.2017.02.155

[21] Caccavo, D. (2019) An overview on the mathematical modeling of hydrogels' behavior for drug delivery systems. *International Journal of Pharmaceutics*. 560, 175–190. https://doi.org/10.1016/j.ijpharm.2019.01.076

[22] Caccavo, D., Cascone, S., Lamberti, G., Barba, A.A. (2015) Controlled drug release from hydrogel-based matrices: Experiments and modeling. *International Journal of Pharmaceutics*. 486(1–2), 144–152. https://doi.org/10.1016/j.ijpharm.2015.03.054

[23] Caccavo, D., Cascone, S., Lamberti, G., Barba, A.A., Larsson, A. (2017a) Drug Delivery From Hydrogels: A General Framework for the Release Modeling. *Current Drug Delivery*. 14, (2), 179–189. http://dx.doi.org/10.2174/1567201813666160808102106

[24] Caccavo, D, Cascone, S., Poto, S., Lamberti, G., Barba, A.A. (2017b) Mechanics and transport phenomena in agarose-based hydrogels studied by compression-relaxation tests. *Carbohydrate Polymers*. 167, 136–144. https://doi.org/10.1016/j.carbpol.2017.03.027

[25] Caccavo, D., Lamberti, G., Barba, A.A. (2020) Mechanics and drug release from poroviscoelastic hydrogels: Experiments and modeling. *European Journal of Pharmaceutics and Biopharmaceutics*. 152, 299–306. https://doi.org/10.1016/j.ejpb.2020.05.020

[26] Cai, S., Lou, Y., Ganguly, P., Robisson, A., Suo, Z. (2010a) Force generated by a swelling elastomer subject to constraint. *Journal of Applied Physics*. 107: 103535. https://doi.org/10.1063/1.3428461

[27] Cai, S., Hu, Y., Zhao, X., Suo, Z. (2010b) Poroelasticity of a covalently crosslinked alginate hydrogel under compression. *Journal of Applied physics*. 108: 113514. https://doi.org/10.1063/1.3517146

[28] Cai, S., Suo, Z. (2011) Mechanics and chemical thermodynamics of phase transition in temperature-sensitive hydrogels. *Journal of the Mechanics and Physics of Solids*. 59(11), 2259–2278. https://doi.org/10.1016/j.jmps.2011.08.008

[29] Cai, S., Suo, Z. (2012) Equations of state for ideal elastomeric gels. *EPL*. 97(3). https://doi.org/10.1209/0295-5075/97/34009

[30] Calderer, M.C., Chabaud, B., Lyu, S., Zhang, H. (2010) Modeling approaches to the dynamics of hydrogel swelling. *Journal of Computational and Theoretical Nanoscience*. 7(4), 766–779. https://doi.org/10.1166/jctn.2010.1419

[31] Caló, E., Khutoryanskiy, V.V. (2015) Biomedical applications of hydrogels: A review of patents and commercial products. *European Polymer Journal*. 65, 252-267. https://doi.org/10.1016/j.eurpolymj.2014.11.024

[32] Charras, G.T., Mitchison, T.J., Mahadevan, L., (2009) Animal cell hydraulics. *Journal of Cell Science*. 122: 3233-3241.

[33] Chester, S.A. (2012) A constitutive model for coupled fluid permeation and large viscoelastic deformation in polymeric gels. *Soft Matter*. 8(31), 8223–8233. https://doi.org/10.1039/c2sm25372k

[34] Chester, S.A., Anand, L. (2010) A coupled theory of fluid permeation and large deformations for elastomeric materials. *Journal of the Mechanics and Physics of Solids*. 58(11), 1879–1906. https://doi.org/10.1016/j.jmps.2010.07.020

[35] Chester, S.A., Anand, L. (2011) A thermo-mechanically coupled theory for fluid permeation in elastomeric materials: Application to thermally responsive gels. *Journal of the Mechanics and Physics of Solids*. 59(10), 1978–2006. https://doi.org/10.1016/j.jmps.2011.07.005

[36] Chung, B.G., Lee, K.H., Khademhosseini, A., Lee, S.H. (2012) Microfluidic fabrication of microengineered hydrogels and their application in tissue engineering. *Lab on a Chip*. 12(1), 45–59. https://doi.org/10.1039/c1lc20859d

[37] Cohen, M.H., Turnbull, D. (1959) Molecular transport in liquids and glasses. *The Journal of Chemical Physics*. 31(5), 1164–1169. https://doi.org/10.1063/1.1730566

[38] Cukier, R.I. (1984) Diffusion of Brownian spheres in semidilute polymer solutions. *Macromolecules*. 17(2), 252–255. https://doi.org/10.1021/ma00132a023

[39] Davidson, G.W., Peppas, N.A. (1986) Solute and penetrant diffusion in swellable polymers. VI. The Deborah and swelling interface numbers as indicators of the order of biomolecular release. *Journal of Controlled Release*. 3(1–4), 259–271. https://doi.org/10.1016/0168-3659(86)90097-0

[40] Deng, G., Li, F., Yu, H., Liu F., Liu C., Sun W., Jiang H., Chen Y. (2012) Dynamic Hydrogels with an Environmental Adaptive Self-Healing Ability and Dual Responsive Sol-Gel Transitions. *ACS Macro Letter*. 1, 275–279. https://doi.org/10.1021/mz200195n

[41] Dimitriyev, M.S., Chang, Y.W., Goldbart, P.M., Fernández-Nieves, A. (2019) Swelling thermodynamics and phase transitions of polymer gels. *Nano Futures*. 3(4), 1–43. https://doi.org/10.1088/2399-1984/ab45d5

[42] Doi, M. (2009) Gel dynamics. *Journal of the Physical Society of Japan*. 78(5), 1–19. https://doi.org/10.1143/JPSJ.78.052001

[43] Doi, M., Onuki, A. (1992) Dynamic coupling between stress and composition in polymer solutions and blends. *Journal de Physique II*. 2(8), 1631–1656. https://doi.org/10.1051/jp2:1992225

[44] Drozdov, A.D. (2014) Swelling of thermo-responsive hydrogels. European Physics Journal E. 37, 1-13. https://doi.org/10.1140/epje/i2014-14093-2

[45] Drozdov, A.D. (2015) Volume phase transition in thermo-responsive hydrogels: Constitutive modeling and structure–property relations. *Acta Mechanica.* 226. 1283–1303. https://doi.org/10.1007/s00707-014-1251-9

[46] Duda, F.P., Souza, A.C., Fried, E. (2010) A theory for species migration in a finitely strained solid with application to polymer network swelling. *Journal of the Mechanics and Physics of Solids*. 58(4), 515–529. https://doi.org/10.1016/j.jmps.2010.01.009

[47] Durning, C.J., Morman, K.N. (1993) Nonlinear swelling of polymer gels. *The Journal of Chemical Physics*. 98(5), 4275–4293. https://doi.org/10.1063/1.465034

[48] Dušek, K., Dušková, M., Ilavský, M., Stewart, R., Kopeček, J. (2003) Swelling pressure induced phase-volume transition in hybrid biopolymer gels caused by unfolding of folded crosslinks: A model. *Biomacromolecules*. 4(6), 1818–1826. https://doi.org/10.1021/bm034219s

[49] Ferreira, J.A., De Oliveira, P., Grassi, M., Romanazzi, G. (2018) Drug Release from Viscoelastic Swelling Polymeric Platforms. *SIAM Journal on Applied Mathematics*. 78(3), 1378–1401. https://doi.org/10.1137/16M1100344

[50] Ferris, C.J., Gilmore, K.J., Wallace, G.G., Panhuis, M.I.H. (2013) Modified gellan gum hydrogels for tissue engineering applications. *Soft Matter*. 9(14), 3705–3711. https://doi.org/10.1039/c3sm27389j

[51] Flory, P.J., Rehner, J. (1943) Statistical mechanics of crosslinked polymer networks I. Rubberlike elasticity. *The Journal of Chemical Physics*. 11(11), 512–520. https://doi.org/10.1063/1.1723791

[52] Fornasiero, F., Prausnitz, J.M., Radke, C.J. (2006) Post-lens tear-film depletion due to evaporative dehydration of a soft contact lens. *Journal of Membrane Science*. 275(1–2), 229–243. https://doi.org/10.1016/j.memsci.2005.09.047

[53] Fornasiero, F., Krull, F., Prausnitz, J.M., Radke, C.J. (2005) Steady-state diffusion of water through soft-contact-lens materials. *Biomaterials*. 26(28), 5704–5716. https://doi.org/10.1016/j.biomaterials.2005.02.028

[54] Fornasiero, F., Tang, D., Boushehri, A., Prausnitz, J.M., Radke, C.J. (2008) Water diffusion through hydrogel membranes. A novel evaporation cell free of external mass-transfer resistance. *Journal of Membrane Science*. 320(1–2), 423–430. https://doi.org/10.1016/j.memsci.2008.04.032

[55] Garcés, V., Palencia, M., Combatt, E. (2017) Development of bacterial inoculums based on biodegradable hydrogels for agricultural applications. *Journal of Science with Technological Applications*. 2, 13-23. https://doi.org/10.34294/j.jsta.17.2.11

[56] García-Arribas, A.B., Axpe, E., Mujika, J.I., Mérida, D., Busto, J.V., Sot, J., Alonso, A., Lopez, X., García, J.A., Ugalde, J.M., Plazaola, F., Goñi, F.M. (2016) Cholesterol-Ceramide Interactions in Phospholipid and Sphingolipid Bilayers As Observed by Positron Annihilation Lifetime Spectroscopy and Molecular Dynamics Simulations. *Langmuir*. 32(21), 5434–5444. https://doi.org/10.1021/acs.langmuir.6b00927

[57] Gerlach, G., Guenther, M., Sorber, J., Suchaneck, G., Arndt, K.F., Richter, A. (2005) Chemical and pH sensors based on the swelling behavior of hydrogels. *Sensors and Actuators, B: Chemical*. 111–112(11), 555–561. https://doi.org/10.1016/j.snb.2005.03.040

[58] Giri, N., Del Pópolo, M.G., Melaugh, G., Greenaway, R.L., Rätzke, K., Koschine, T., Pison, L., Gomes, M.F.C., Cooper, A. I., James, S.L. (2015) Liquids with permanent porosity. *Nature*. 527(7577), 216–220. https://doi.org/10.1038/nature16072

[59] Gurtin, M. E., Fried, E., Anand, L. V – Basic thermodynamical principles. X – Mechanical theory of elastic solids. XII – Species diffusion coupled to elasticity. The Mechanics and Thermodynamics of Continua. *Cambridge University Press*. (2010), 181-206, 271-330, 331-414. https://doi.org/10.1017/cbo9780511762956

[60] Gyun-Nam, H., Gyun-Nam, M., Yoo, P.J., Kim, J.H. (2019) Hydrogen bonding-based strongly adhesive coacervate hydrogels synthesized using poly(N-vinylpyrrolidone) and tannic acid. *Soft Matter*. 15, 785-791. https://doi.org/10.1039/C8SM02144A

[61] Hadjiev, N.A., Amsden, B.G. (2015) An assessment of the ability of the obstruction-scaling model to estimate solute diffusion coefficients in hydrogels. *Journal of Controlled Release*. 199, 10–16. https://doi.org/10.1016/j.jconrel.2014.12.010

[62] Hagel, V., Haraszti, T., Boehm, H. (2013) Diffusion and interaction in PEG-DA hydrogels. *Biointerphases*. 8(1), 1–9. https://doi.org/10.1186/1559-4106-8-36

[63] Han, Y.I., Hong, W.E., Faidley, L., (2011) Couple magnetic field and viscoelasticity of ferrogel. International *Journal of Applied Mechanics*. 3, 259-278. https://doi.org/10.1142/S175882511100097X

[64] Hansing, J., Netz, R.R. (2018) Hydrodynamic Effects on Particle Diffusion in Polymeric Hydrogels with Steric and Electrostatic Particle-Gel Interactions. *Macromolecules*. 51(19), 7608–7620. https://doi.org/10.1021/acs.macromol.8b01494

[65] He, T., Li, M., Zhou, J. (2012) Modeling deformation and contacts of pH sensitive hydrogels for microfluidic flow control. *Soft Matter*. 8(11), 3083–3089. https://doi.org/10.1039/c2sm06749h

[66] Hoare, T.R., Kohane, D.S. (2008) Hydrogels in drug delivery: Progress and challenges. *Polymer*. 49(8), 1993–2007. https://doi.org/10.1016/j.polymer.2008.01.027

[67] Holzapfel, G. (2002) Nonlinear Solid Mechanics: A Continuum Approach for Engineering Science. *Meccanica*. 37(4–5). https://doi.org/10.1023/A:1020843529530

[68] Hong, W., Zhao, X., Suo, Z. (2010) Large deformation and electrochemistry of polyelectrolyte gels. *Journal of the Mechanics and Physics of Solids*. 58(4), 558–577. https://doi.org/10.1016/j.jmps.2010.01.005

[69] Hong, W., Zhao, X., Zhou, J., Suo, Z. (2008) A theory of coupled diffusion and large deformation in polymeric gels. *Journal of the Mechanics and Physics of Solids*. 56(5), 1779–1793. https://doi.org/10.1016/j.jmps.2007.11.010

[70] Hu, Y., Suo, Z. (2012) Viscoelasticity and poroelasticity in elastomeric gels. *Acta Mechanica Solida Sinica*. 25(5), 441–458. https://doi.org/10.1016/S0894-9166(12)60039-1

[71] Hu, Y., Chen, X., Whitesides, G.M., Vlassak, J.J., Suo, Z. (2011) Indentation of polydimethylsiloxane submerged in organic solvents. *Journal of Material Reaserch*. 26: 785-795. https://doi.org/10.1557/jmr.2010.35

[72] Hu, Y., Zhao, X., Vlassak, J.J., Suo, Z. (2010) Usingin dentation to characterize the poroelasticity of gels. *Applied physics Letters*, 96: 121904. https://doi.org/10.1063/1.3370354

[73] Huggins, M.L. (1941) Solutions of long chain compounds. *The Journal of Chemical Physics*. 9(5), 440. https://doi.org/10.1063/1.1750930

[74] Hui, C.Y., Lin, Y.Y., Chuang, F.U.C., Shull, K.R., Lin, W.C. (2006) A contact mechanics method for characterizing the elastic properties and permeability of gels. *Journal of Polymer Science, Part B: Polymer Physics*. 44(2), 359–370. https://doi.org/10.1002/polb.20613

[75] Kapur, V., Charkoudian, J.C., Kessler, S.B., Anderson, J.L. (1996) Hydrodynamic permeability of hydrogels stabilized within porous membranes. *Industrial and Engineering Chemistry Research*. 35(9), 3179–3185. https://doi.org/10.1021/ie960015z

[76] Kiszka, M.B., Meilchen, M.A., McHugh, M.A. (1988) Modeling high-pressure gas–polymer mixtures using the sanchez-lacombe equation of state. *Journal of Applied Polymer Science*. 36(3), 583–597. https://doi.org/10.1002/app.1988.070360311

[77] Kotera, K., Saito, T., Yamanaka, T. (2005) Measurement of positron lifetime to probe the mixed molecular states of liquid water. *Physics Letters, Section A: General, Atomic and Solid State Physics*. 345(1–3), 184–190. https://doi.org/10.1016/j.physleta.2005.07.018

[78] Krishna, R., Wesselingh, J.A. (1997) The Maxwell-Stefan approach to mass transfer. *Chemical Engineering Science*. 52(6), 861–911. https://doi.org/https://doi.org/10.1016/S0009-2509(96)00458-7

[79] Kubaczka, A. (2014) Prediction of Maxwell-Stefan diffusion coefficients in polymer-multicomponent fluid systems. *Journal of Membrane Science*. 470, 389–398. https://doi.org/10.1016/j.memsci.2014.06.055

[80] Lee, K.Y., Mooney, D.J. (2001) Hydrogels for tissue engineering. *Chemical Reviews*. 101(7), 1869–1879. https://doi.org/10.1021/cr000108x

[81] Lerma, T., Martinez, G., Palencia, M. (2017) Generation of thiolated porous surfaces by interpenetrating polymeric networks: study of their surface properties. *Journal of Science with Technological Applications*. 3, 56-65. https://doi.org/10.34294/j.jsta.17.3.244

[82] Lerma, T.A., Palencia M., Combatt E.M. (2011) Soil polymer conditioner based on montmorillonite-poly(acrylic acid) composites. *Journal of Applied Polymer Science*. 135, 46211. https://doi.org/10.1002/app.462111

[83] Li, J., Hu, Y., Vlassak, J.J., Suo, Z. (2012) Experimental determination of equations of state for ideal elastomeric gels. *Soft Matter*. 8(31), 8121–8128. https://doi.org/10.1039/c2sm25437a

[84] Li, J., Mooney, D.J. (2016) Designing hydrogels for controlled drug delivery. *Nature Reviews Materials*. 1(12), 1–18. https://doi.org/10.1038/natrevmats.2016.71

[85] Liao, J., Huang, J., Wang, T., Sun, W., Tong, Z. (2017) Rapid shape memory and pH-modulated spontaneous actuation of dopamine containing hydrogels. *Chinese Journal of Polymer Science volume*. 35, 1297–1306. https://doi.org/10.1007/s10118-017-1991-99

[86] Liu, X., Bardow, A., Vlugt, T.J.H. (2011) Multicomponent maxwell-stefan diffusivities at infinite dilution. *Industrial and Engineering Chemistry Research*. 50(8), 4776–4782. https://doi.org/10.1021/ie102515w

[87] Liu, Z., Toh, W., Ng, T.Y. (2015) Advances in Mechanics of Soft Materials: A Review of Large Deformation Behavior of Hydrogels. *International Journal of Applied Mechanics*. 7(5), 1–35. https://doi.org/10.1142/S1758825115300011

[88] Lucantonio, A., Nardinocchi, P., Teresi, L. (2013) Transient analysis of swelling-induced large deformations in polymer gels. *Journal of the Mechanics and Physics of Solids*. 61(1), 205–218. https://doi.org/10.1016/j.jmps.2012.07.010

[89] Luo, Y., Shoichet, M.S. (2004) A photolabile hydrogel for guided three-dimensional cell growth and migration. *Nature Materials*. 3(4), 249–254. https://doi.org/10.1038/nmat1092

[90] Lustig, S.R., Peppas, N.A. (1988) Solute diffusion in swollen membranes. IX. Scaling laws for solute diffusion in gels. *Journal of Applied Polymer Science*. 36(4), 735–747. https://doi.org/10.1002/app.1988.070360401

[91] Mackie, J.S., Meares, P. (1955) The diffusion of electrolytes in a cation-exchange resin membrane. II. Experimental. *Proceedings of the Royal Society of London. Series A. Mathematical and Physical Sciences*. 232(1191), 510–518. https://doi.org/10.1098/rspa.1955.0235

[92] Maitra, J., Shukla, V.K. (2014) Cross-linking in Hydrogels - A Review. *American Journal of Polymer Science*, *4*(2), 25–31. https://doi.org/10.5923/j.ajps.20140402.01

[93] Marcombe, R., Cai, S., Hong, W., Zhao, X., Lapusta, Y., Suo, Z., (2010) A theory of constrained swelling of a pH-sensitive hydrogel. *Soft Matter*. 6, 784-793. https://doi.org/10.1039/B917211D

[94] Noll, W., Coleman, B.D., Noll, W. (1974) The Thermodynamics of Elastic Materials with Heat Conduction and Viscosity. *The Foundations of Mechanics and Thermodynamics*. 145–156. https://doi.org/10.1007/978-3-642-65817-4_9

[95] Offeddu, G.S., Axpe, E., Harley, B.A.C., Oyen, M.L. (2018) Relationship between permeability and diffusivity in polyethylene glycol hydrogels. *AIP Advances*. 8(10). https://doi.org/10.1063/1.5036999

[96] Okay, O., Sariişik, S.B., Zor, S.D. (1998) Swelling behavior of anionic acrylamide-based hydrogels in aqueous salt solutions: Comparison of experiment with theory. *Journal of Applied Polymer Science*. 70(3), 567–575. https://doi.org/10.1002/(SICI)1097-4628(19981017)70:3<567::AID-APP19>3.0.CO;2-Y

[97] Oliveira, E.D., Silva, A.F.S., Freitas, R.F.S. (2004) Contributions to the thermodynamics of polymer hydrogel systems. *Polymer*. 45(4), 1287–1293. https://doi.org/10.1016/j.polymer.2003.11.048

[98] Palencia, M., Mora, M.A., Palencia, S.L. (2017a) Biodegradable Polymer Hydrogels Based in Sorbitol and Citric Acid for Controlled Release of Bioactive Substances from Plants (Polyphenols). *Current Chemical Biology*. 11(1), 36-46 https://doi.org/10.2174/2212796810666161028114432

[99] Palencia, M., Lerma, T.A., Combatt, E.M. (2017b) Hydrogels Based in Cassava Starch with Antibacterial Activity for Controlled Release of Cysteamine-silver Nanostructured Agents. *Current Chemical Biology*. 11(1) 28-35 https://doi.org/10.2174/2212796810666161108152319

[100] Palencia, M., Vera, M., Rivas, B.L. (2014) Modification of ultrafiltration membranes via interpenetrating polymer networks for removal of boron from aqueous solution.*Journal of Membrane Science*. 466, 192-199. http://dx.doi.org/10.1016/j.memsci.2014.05.0033

[101] Peters, A., Candau, S.J. (1986) Kinetics of Swelling. *Macromolecules*. 19, 1952–1955.

[102] Peters, A., Candau, S.J. (1988) Kinetics of Swelling of Spherical and Cylindrical Gels. *Macromolecules*. 21(7), 2278–2282. https://doi.org/10.1021/ma00185a068

[103] Pichioni F., Muljana H. (2018) Hydrogels Based on Dynamic Covalent and Non Covalent Bonds: A Chemistry Perspective. *Gels*. 4 (1), 21. http://dx.doi.org/10.3390/gels40100211

[104] Ricka, J., Tanaka, T., (1984) Swelling of ionic gels: Quantitative performance of the Donnan theory. *Macromolecules*. 17, 2916-2921. https://doi.org/10.1021/ma00142a081

[105] Ribeiro, C.P., Freeman, B.D., Paul, D.R. (2011) Modeling of multicomponent mass transfer across polymer films using a thermodynamically consistent formulation of the Maxwell-Stefan equations in terms of volume fractions. *Polymer*. 52(18), 3970–3983. https://doi.org/10.1016/j.polymer.2011.06.042

[106] Richter, A., Paschew, G., Klatt, S., Lienig, J., Arndt, K.F., Adler, H.J.P. (2008) Review on hydrogel-based pH sensors and microsensors. *Sensors*. 8(1), 561–581. https://doi.org/10.3390/s8010561

[107] Rosenbluth, M.J., Crow, A., Shaevitz, J.W., Fletcher, D.A., (2008) Slow stress propagation in adherent cells. 95: 6052-6059. https://doi.org/10.1529/biophysj.108.139139

[108] Sanchez, I.C., Lacombe, R.H. (1978) Statistical Thermodynamics of Polymer Solutions. *Macromolecules*. 11(6), 1145–1156. https://doi.org/10.1021/ma60066a017

[109] Satarkar, N.S., Biswal, D., Hilt, J.Z. (2010) Hydrogel nanocomposites: A review of applications as remote controlled biomaterials. *Soft Matter*. 6(11), 2364–2371. https://doi.org/10.1039/b925218p

[110] Schapery, R.A., (1997) Nonlinear Viscoelastic and Viscoplastic Constitutive Equations Based on Thermodynamics, *Mechanics of Time-Dependent Materials*. 1:209-240. https://doi.org/10.1023/A:1009767812821

[111] Siepmann, J., Siepmann, F. (2012) Modeling of diffusion controlled drug delivery. *Journal of Controlled Release*. 161(2), 351–362. https://doi.org/10.1016/j.jconrel.2011.10.006

[112] Snoeijer J. H., Pandey A., Herrada M. A. and Eggers J. (2020) The relationship between viscoelasticity and elasticity. *Proc. R. Soc. A*. 476: 20200419. 20200419. https://doi.org/10.1098/rspa.2020.0419

[113] Strange, D.G., Fletcher, T.L., Tonsomboon, K., Brawn, H., Zhao, X., Oyen, M.L., (2013) Separating poroviscoelastic deformation mechanisms in hydrogels. A*pplied Physics Letters*. 102, 031913. https://doi.org/10.1063/1.4789368

[114] Suo, Z. (2010) Theory of dielectric elastomers. *Acta Mechanica Solida Sinica*. 23(6), 549–578. https://doi.org/10.1016/S0894-9166(11)60004-9

[115] Tanaka, T., Fillmore, D.J. (1979) Kinetics of swelling of gels. *The Journal of Chemical Physics*. 70(3), 1214–1218. https://doi.org/10.1063/1.437602

[116] Tanaka, T., Hocker, L.O., Benedek, G.B. (1973) Spectrum of light scattered from a viscoelastic gel. *The Journal of Chemical Physics*. 59(9), 5160–5183. https://doi.org/10.1063/1.1680734

[117] Taylor, R., Krishna, R. 2 – The Maxwell – Stefan Relations. 3 – Fick's Law. Multicomponent Mass Transfer. *John Wiley & Sons, Inc.* (1993) 13 – 49. ISBN: 978-0-471-57417-0. https://books.google.com.co/books?id=FrpX9dNjWc0C

[118] Van Vlierberghe, S., Dubruel, P., Schacht, E. (2011) Biopolymer-based hydrogels as scaffolds for tissue engineering applications: A review. *Biomacromolecules*. 12(5), 1387–1408. https://doi.org/10.1021/bm200083n

[119] Vrentas, J.S., Duda, J.L. (1977) Diffusion in Polymer-Solvent Systems - 3. Construction of Deborah Number Diagrams. *J Polym Sci Polym Phys Ed*. 15(3), 441–453. https://doi.org/10.1002/pol.1977.180150304

[120] Vrentas, J.S., Jarzebski, C.M., Duda, J.L. (1975) A Deborah number for diffusion in polymer-solvent systems. *AIChE Journal*. 21(5), 894–901. https://doi.org/10.1002/aic.690210510

[121] Wang, Q.M., Mohan, A.C., Oyen, M.L., Zhao, X.H. (2014) Separating viscoelasticity and poroelasticity of gels with different length and time scales. *Acta Mechanica Sinica*. 30(1), 20–27. https://doi.org/10.1007/s10409-014-0015-z

[122] Wang, X., Hong, W. (2012) A visco-poroelastic theory for polymeric gels. *Proceedings of the Royal Society A: Mathematical, Physical and Engineering Sciences*. 468(2148), 3824–3841. https://doi.org/10.1098/rspa.2012.0385

[123] Xu, Q., Huang, W., Jiang, L., Lei, Z., Li, X., et al. (2013) KGM and PMAA based pH-sensitive interpenetrating polymer network hydrogel for controlled drug release. *Carbohydrate Polymers.* 97, 565-570. https://doi.org/10.1016/j.carbpol.2013.05.007

[124] Yamaue, T., Doi, M. (2004) Theory of one-dimensional swelling dynamics of polymer gels under mechanical constraint. *Physical Review E - Statistical Physics, Plasmas, Fluids, and Related Interdisciplinary Topics*. 69(4), 5. https://doi.org/10.1103/PhysRevE.69.041402

[125] Yamaue, T., Doi, M. (2005) The stress diffusion coupling in the swelling dynamics of cylindrical gels. *Journal of Chemical Physics*. 122(8). https://doi.org/10.1063/1.1849153

[126] Yan, H., Jin, B., Gao, S., Chen, L., (2014) Equilibrium swelling and electrochemistry of polyampholytic pH-sensitive hydrogel. *International Journal of Solids and Structures*. 51, 4149-4156.

[127] Yoon, J., Cai, S., Suo, Z., Hayward, R.C. (2010) Poroelastic swelling kinetics of thin hydrogel layers: Comparison of theory and experiment. *Soft Matter*. 6(23), 6004–6012. https://doi.org/10.1039/c0sm00434k

[128] Zhao, J., Chen, Y., Ying, Y., Zong-Rui, T., et al. (2018) Preparation of the polyelectrolyte complex hydrogel of biopolymers via a semi-dissolution acidification sol-gel transition method and its application in solid-state supercapacitors. *Journal of Power Sources*. 378, 603-609. https://doi.org/10.1016/j.jpowsour.2018.01.005

[129] Zhao, X., Huebsch, N., Mooney, D.J., Suo, Z., (2010) Stress-relaxation behavior in gels with ionic and covalent crosslinks. *Journal of Applied Physics.* 107: 063509. https://doi.org/10.1063/1.3343265

[130] Zhao, X., Kim, J., Cezar, C.A., Huebsch, N., Lee, K., Bouhadir, K., Mooney, D.J. (2011) Active scaffolds for on-demand drug and cell delivery. *Proceedings of the National Academy of Sciences of the United States of America*. 108(1), 67–72. https://doi.org/10.1073/pnas.1007862108